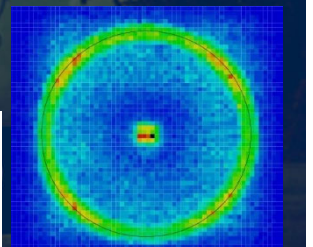
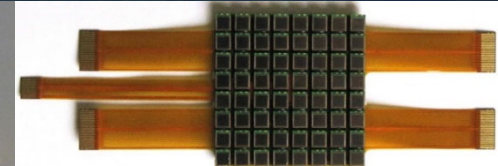
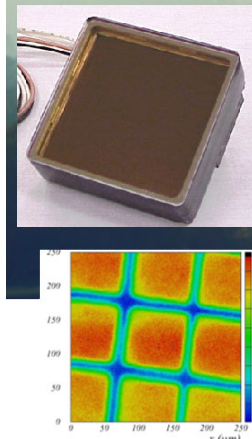


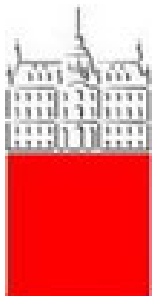
The 13th International Conference on Position Sensitive Detectors PSD13

St. Catherine's College, Oxford, September 3-8, 2023

PSD13



Novel photon detectors



Peter Križan

University of Ljubljana and J. Stefan Institute



Introduction: why?

Photon detectors are at the heart of most experiments in particle physics. Moreover, they are also finding application in other scientific fields (chemistry and biology) and are ubiquitous in society in general.

New environments where we need to detect light (in particular low light levels)
→ need advances in existing technology and transformative, novel ideas to meet the demanding requirements.

Two main lines of R&D to be pursued have been identified by the ECFA Detector R&D Roadmap:

- Enhance timing resolution and spectral range of photon detectors.
- Develop photosensors for extreme environments.

This talk: photosensors will be discussed in this spirit; also: the main emphasis will be on low light level detection.

Contents

Introduction: why and what kind of photosensor?

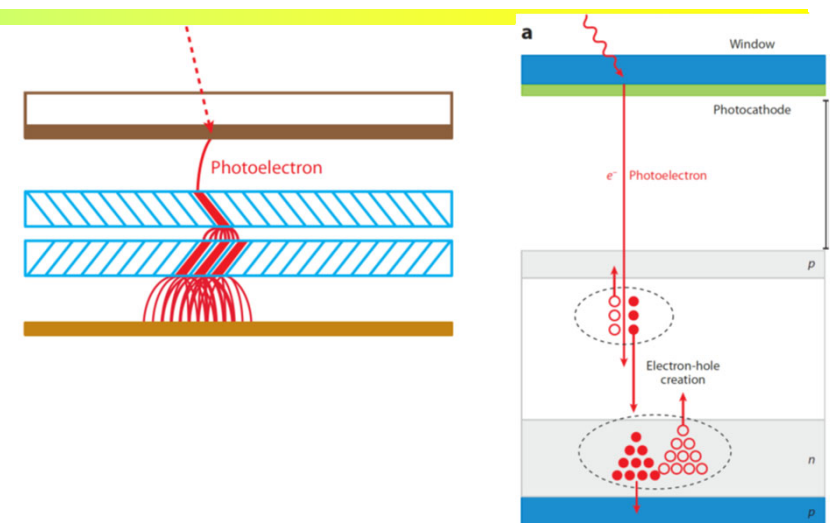
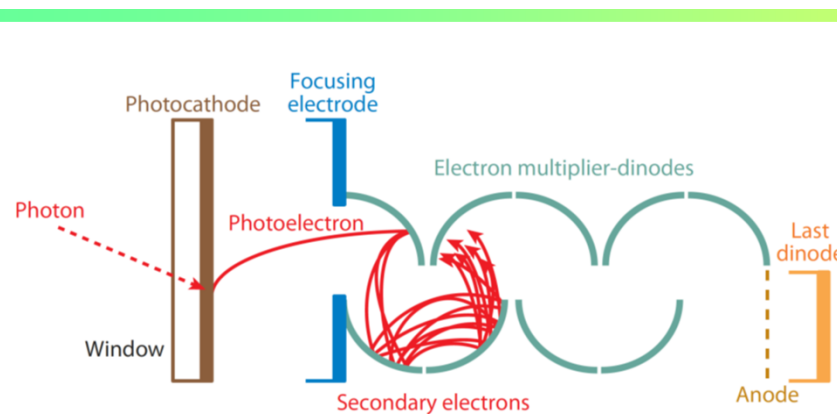
Vacuum-based photodetectors

Solid state low light level photosensors

Gas-based photodetectors

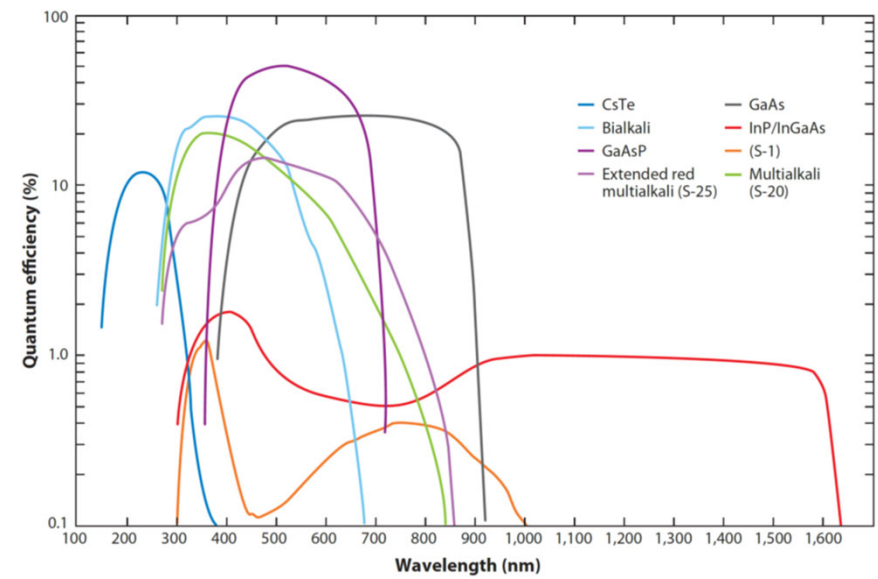
Summary and outlook

Vacuum-based photodetectors

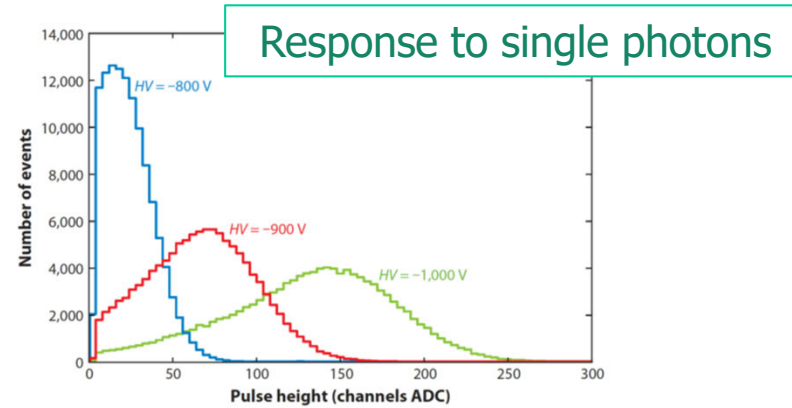
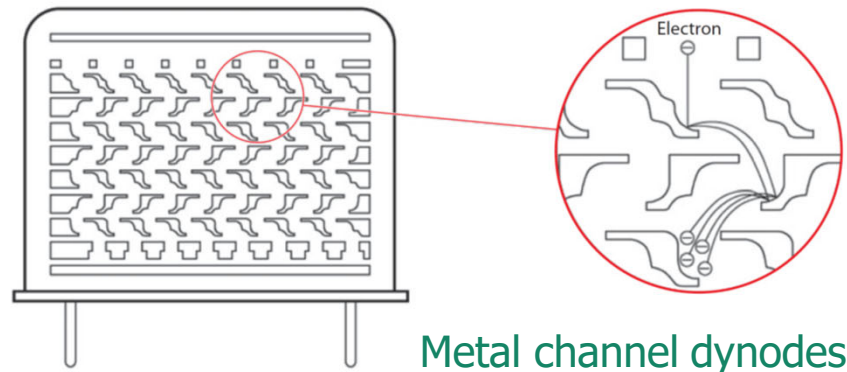


Generic steps:

- Photon → photoelectron conversion
- Photoelectron collection in the multiplication system
- Multiplication (dynodes, microchannel plates, high E field + Si)
- Signal collection

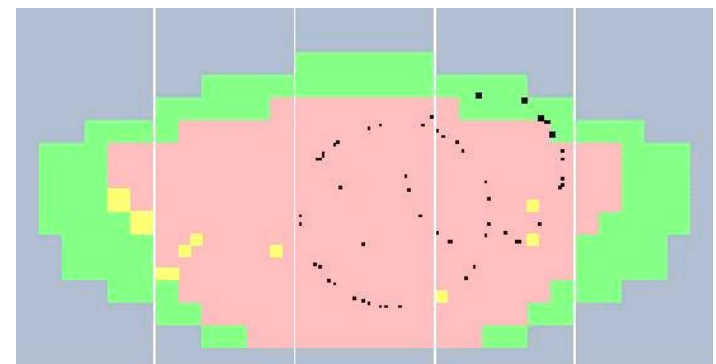


Multianode photomultiplier tubes (PMTs)



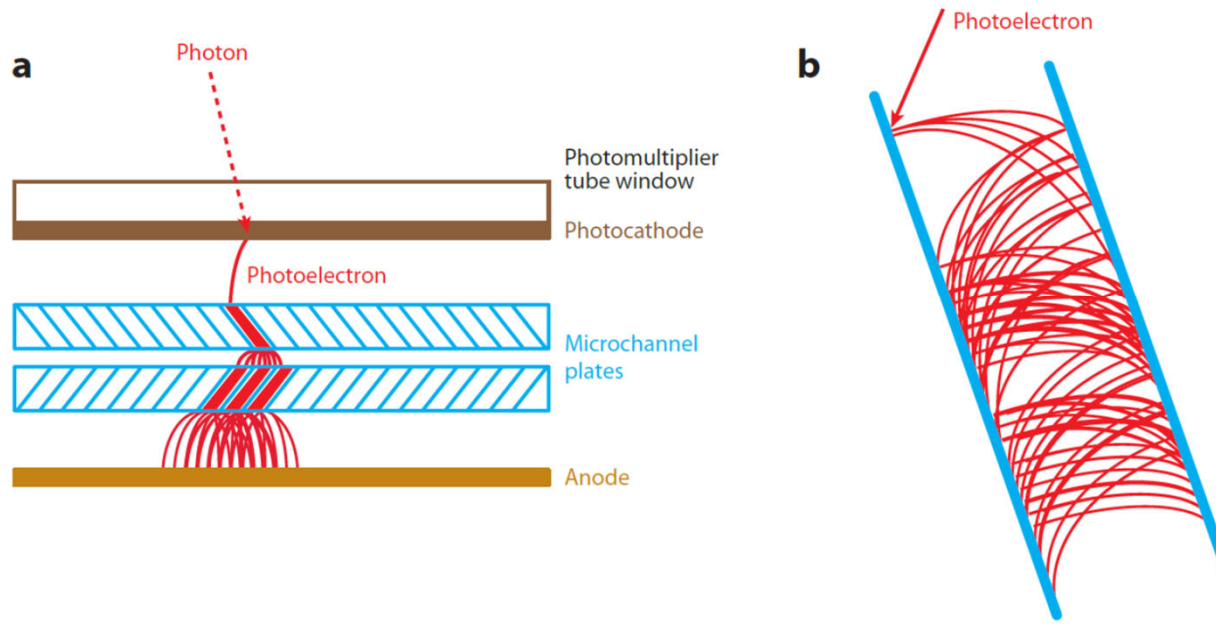
Pioneered in the HERA-B RICH, later used in the COMPASS, CLASS12 and GlueX RICH detectors

Recent use in the upgraded LHCb RICH detectors; planned for CBM RICH



Excellent performance (excellent single photon detection efficiency, very low noise, low cross-talk), best choice for large areas with no B field

Micro Channel Plate PMT (MCP-PMT)



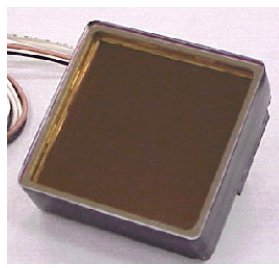
Multiplication step: a continuous dynode – a micro-channel

Micro Channel Plate PMT (MCP-PMT)

Similar to ordinary PMT – the dynode structure is replaced by MCPs.

Basic characteristics:

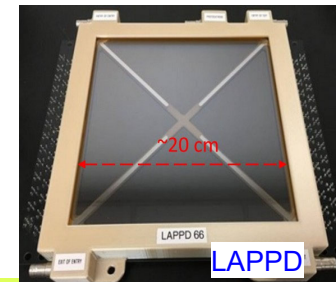
- Gain $\sim 10^6$ → single photon
- Collection efficiency $\sim 60\%$
- Small thickness, high field → small TTS
- Works in magnetic field
- Segmented anode
→ position sensitive



PHOTONIS

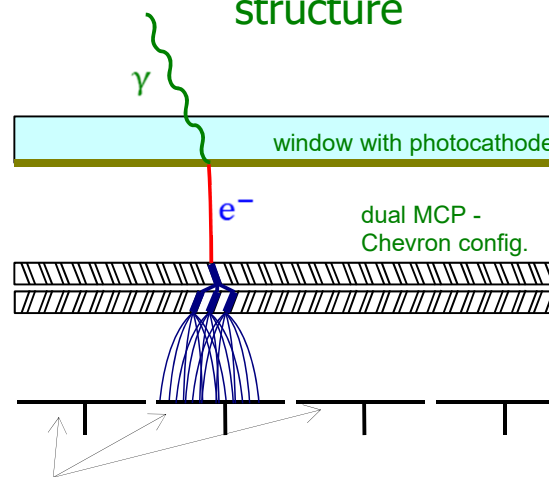


PHOTEK

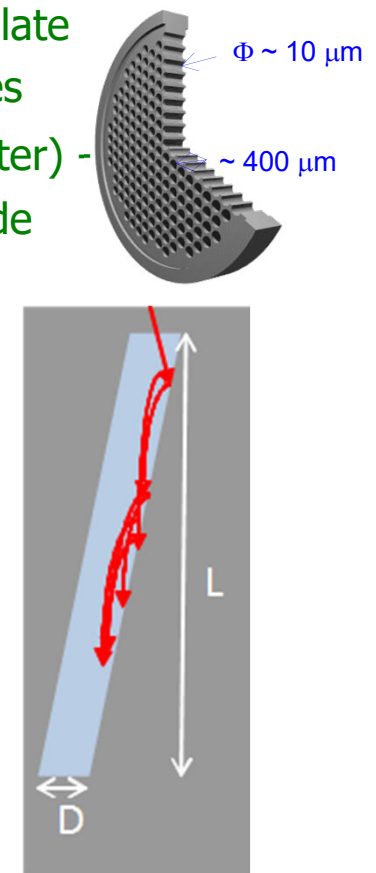


PSD13

MCP is a thin glass plate with an array of holes ($<10-100 \mu\text{m}$ diameter) -
- a continuous dynode structure



Anodes → can be segmented according to application needs



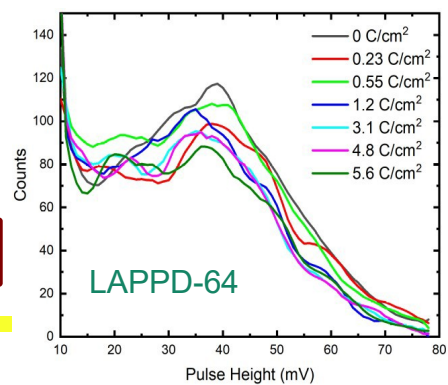
MCP gain depends on L/D ratio – typically 1000 for L/D=40

MCP PMT ageing

MCP PMTs: photo-cathode degradation due to ion feedback, main concern in high intensity experiments

ALD (atomic layer deposition) coating of MCP pores → ~100x photo-cathode lifetime increase

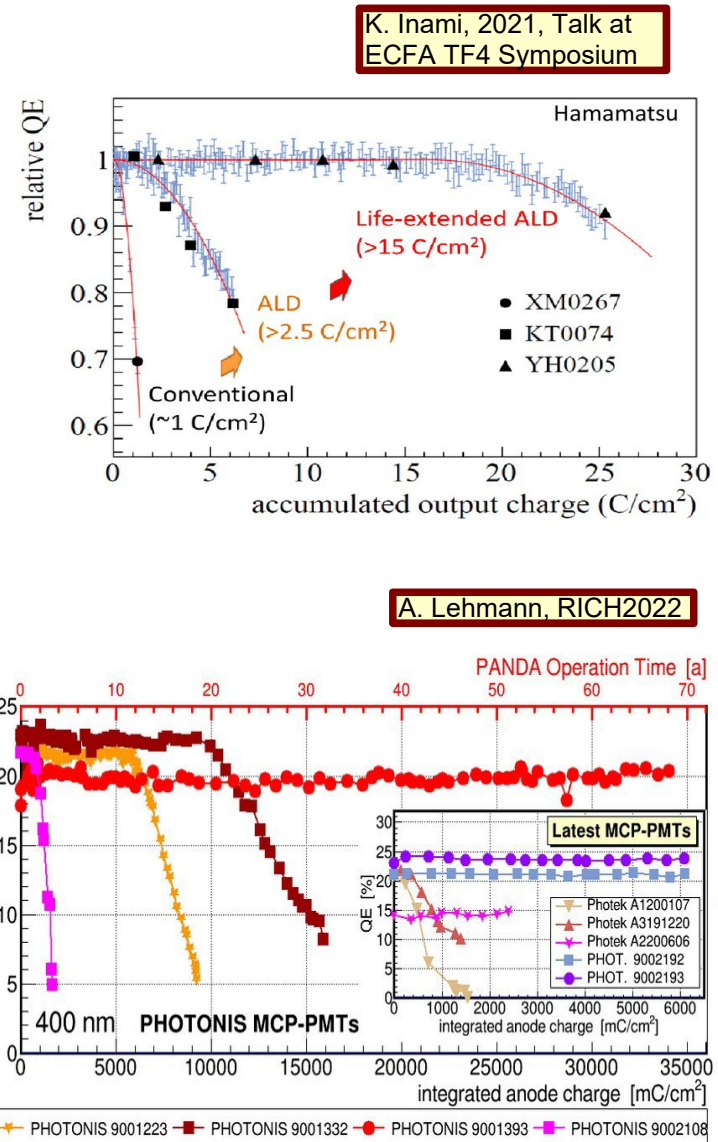
- Hamamatsu 1-inch YH0205 ($>20 \text{ C/cm}^2$) [K. Inami, 2021]
- No QE degradation for Photonis MCP-PMT (R2D2) to $>34 \text{ C/cm}^2$
- Little QE degradation in LAPPD 8-inch up to 5.6 C/cm^2 [V. A. Chirayath, CPAD2021]



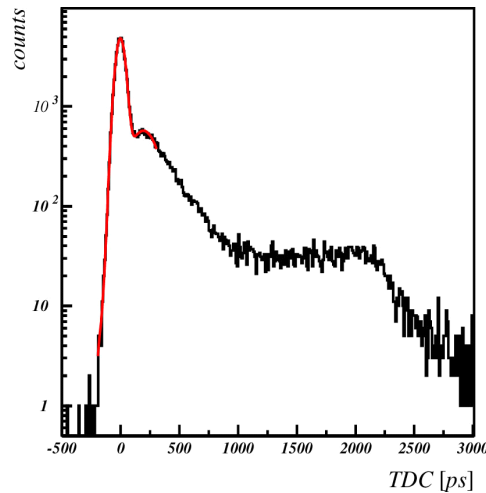
V.A. Chirayath et al.,
Talk at CPAD 2021

Sept. 4, 2023

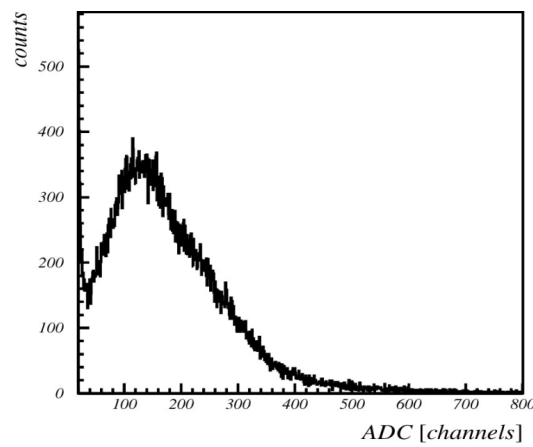
PSD13



MCP-PMT: single photon pulse height and timing



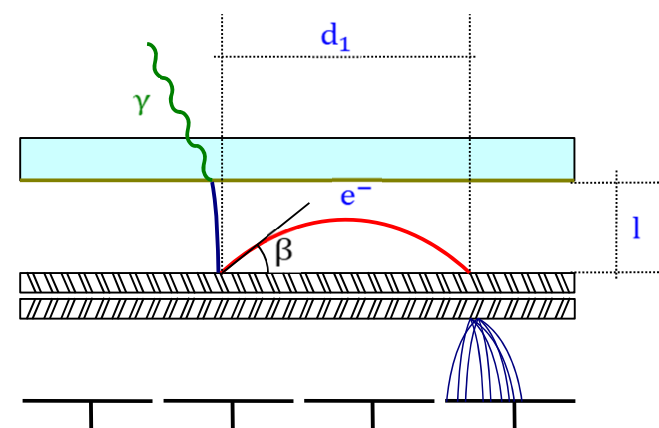
Typical single photon timing distribution with a narrow main peak ($\sigma \sim 40$ ps) and contributions from photoelectron elastic (flat distribution) and inelastic back-scattering.



Gain in a single channel saturates at high gains due to space charge effect → peaking distribution for single photoelectrons

Photoelectron back-scattering produces a rather long tail in timing distribution and position resolution.

Photoelectron backscattering reduces collection efficiency and gain, and contributes to cross-talk in multi-anode PMTs



S.Korpar@PD07

Photoelectron in uniform electric field

Photoelectrons travel from photocathode to the electron multiplier (uniform electric field $\frac{U}{l}$, initial energy $E_0 \ll Ue_0$):

- photoelectron range

$$d_0 \approx 2l \sqrt{\frac{E_0}{Ue_0}} \sin(\alpha)$$

- and maximal travel time (sideway start)

$$t_0 \approx l \sqrt{\frac{2m_e}{Ue_0}}$$

- time difference between downward and sideways initial direction

$$\Delta t \approx t_0 \sqrt{\frac{E_0}{Ue_0}}$$

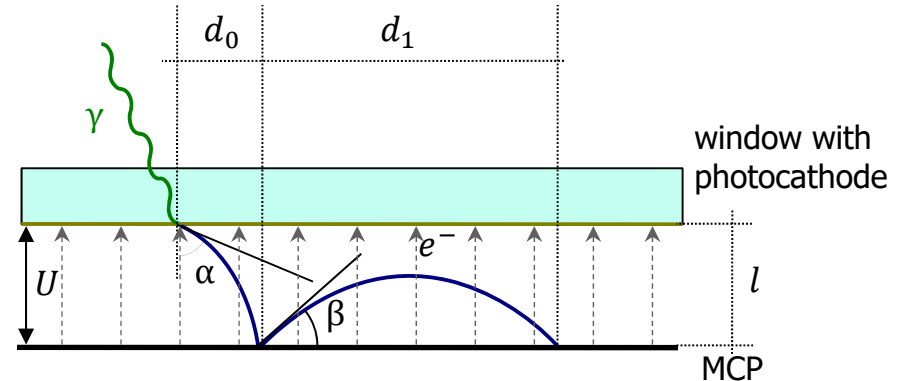
Example ($U = 200 \text{ V}$, $E_0 = 1 \text{ eV}$, $l = 6 \text{ mm}$)

photoelectron:

- max range $d_0 \approx 0.8 \text{ mm}$
- p.e. transit time $t_0 \approx 1.4 \text{ ns}$
- $\Delta t \approx 100 \text{ ps}$

backscattering:

- max range $d_1 = 2l = 12 \text{ mm}$
- max delay $t_1 = 2.8 \text{ ns}$



Backscattering delay and range (maximum for elastic scattering):

- maximum range vs. angle

$$d_1 = 2l \sin(2\beta)$$

maximum range for backscattered photoelectron is twice the photocathode – first electrode distance

- maximum delay vs. angle

$$t_1 = 2t_0 \sin(\beta)$$

maximum delay is twice the photoelectron travel time

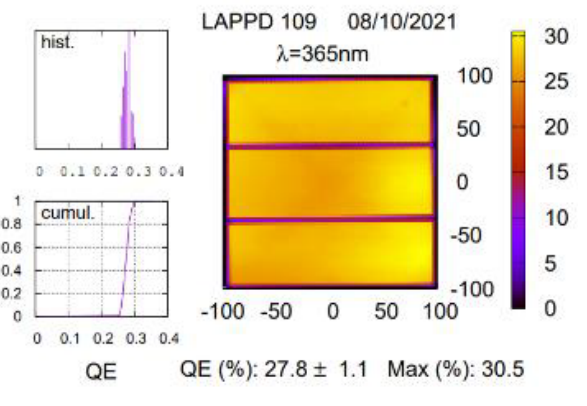
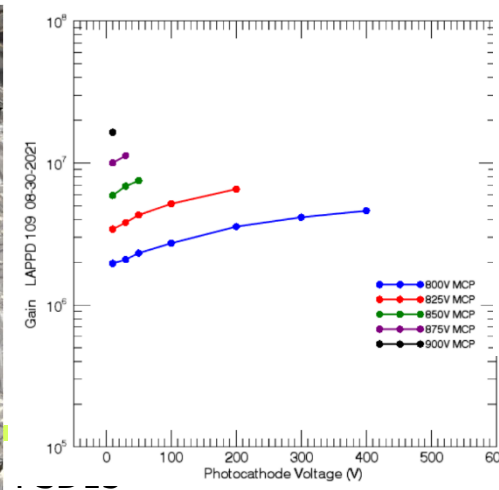
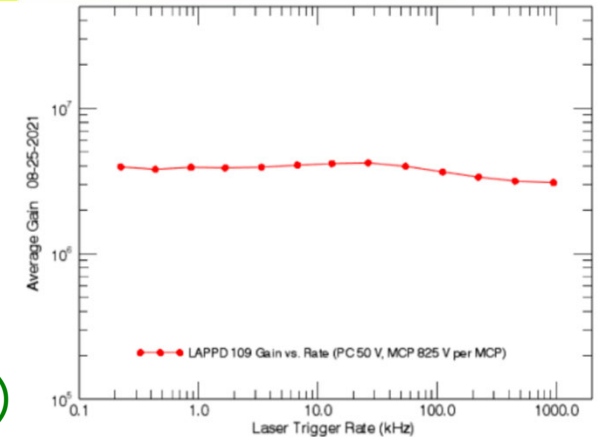
- time of arrival of elastically scattered photoelectrons: flat distribution up to max $t_1 = 2t_0$

S.Korpar@PD07

LAPPD (large area picosecond photodetector) Gen II

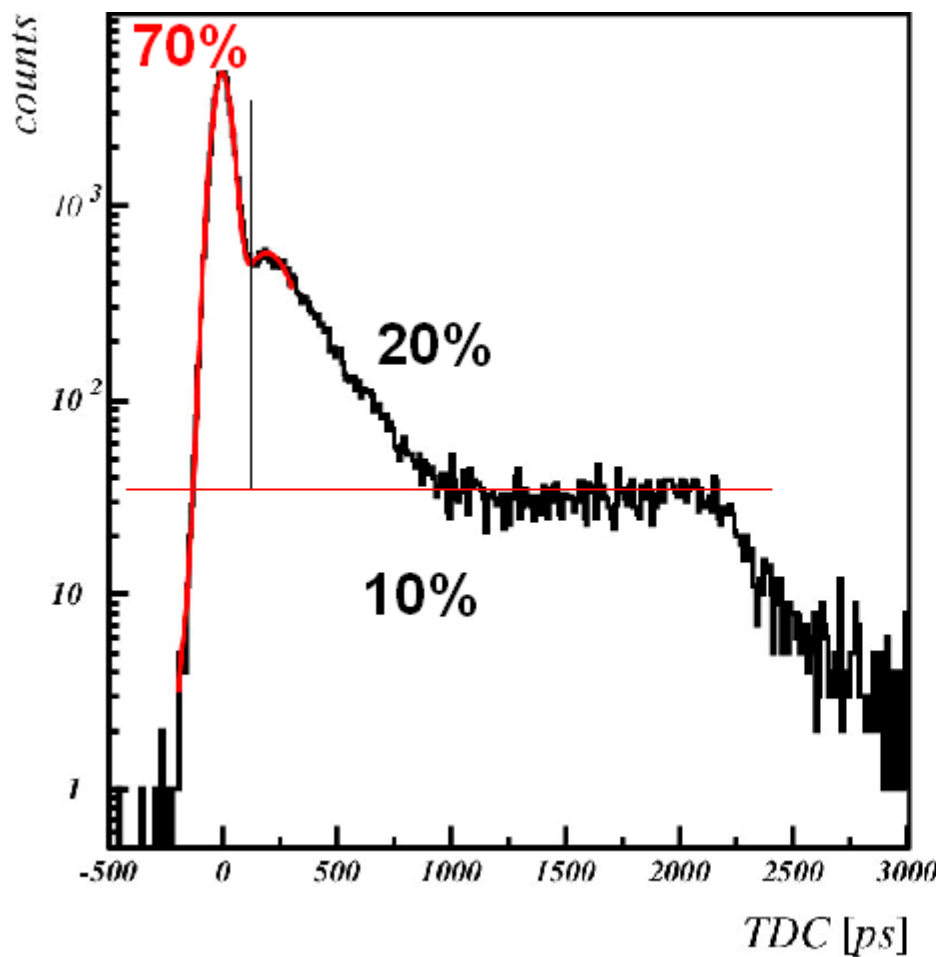
Characteristics (Incom):

- borosilicate back plate with interior resistive ground plane
anode – 5 mm thick
- capacitively coupled readout electrode
- MCPs with $20 \mu\text{m}$ pores at $20 \mu\text{m}$ pitch
- two parallel spacers (active fraction $\approx 97 \%$)
- gain $\approx 5 \cdot 10^6$ @ ROP (825 V/MCP, 100 V on photocathode)
- peak QE $\approx 25\%$
- size 230 mm x 220 mm x 22 mm (243 mm X 274 mm X 25.2 mm with mounting case)
- Dark Count rate @ ROP: $\sim 70 \text{ kHz/cm}^2$ with 8×10^5 gain



Peter Križan, Ljubljana

MCP PMT timing



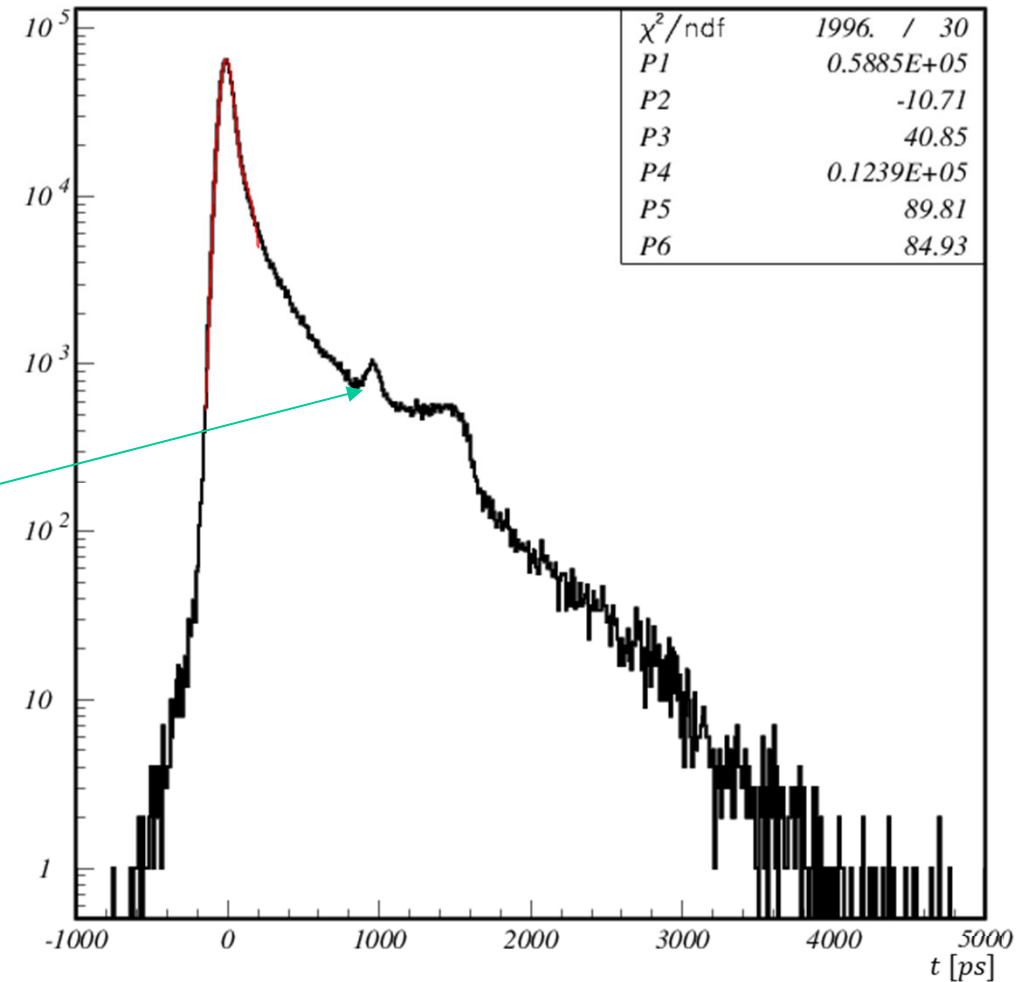
Tails understood (elastic and inelastic scattering of photoelectrons off the MCP), can be significantly reduced by:

- decreased photocathode-MCP distance and
- increased voltage difference

- prompt signal $\sim 70\%$
- short delay $\sim 20\%$
- $\sim 10\%$ uniform distribution

LAPPD – timing distribution

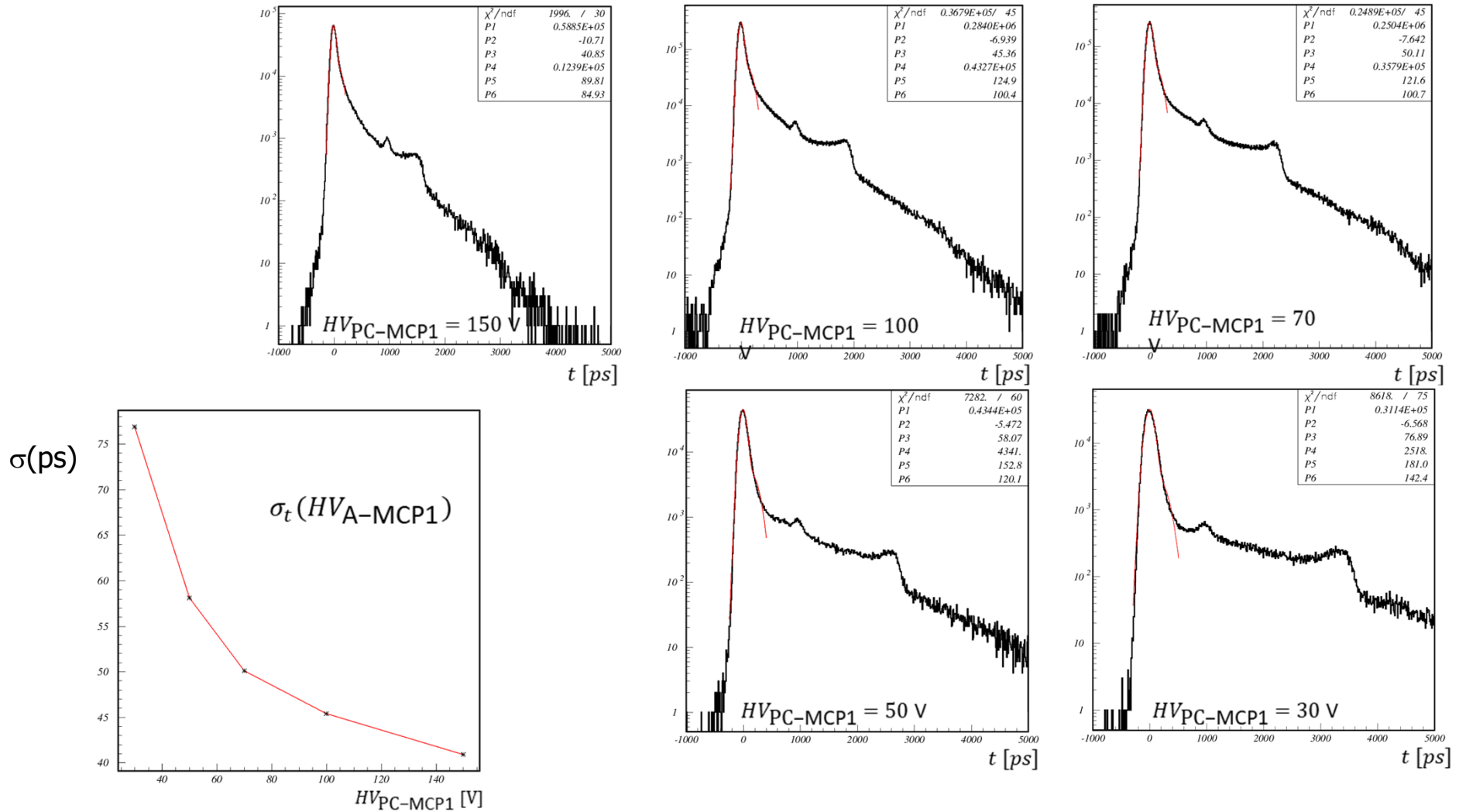
- measured timing distribution typical for MCP-PMT
- main prompt peak with some inelastic and elastic backscattering contribution
- additional small peak at about 1 ns delay probably due to some reflection (light?), delay not affected by PC-MCP1 voltage
- The plot is for the PC-MCP1 voltage of 150 V and recommended HV for others



S. Korpar et al., to be
submitted to NIMA

LAPPD – timing vs PC-MCP1 voltage

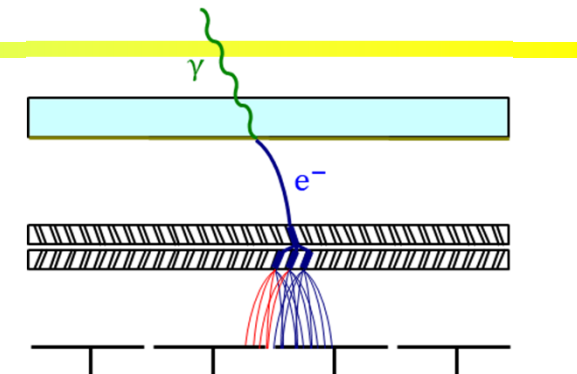
Time-walk corrected TDCs for different PC-MCP1 voltages



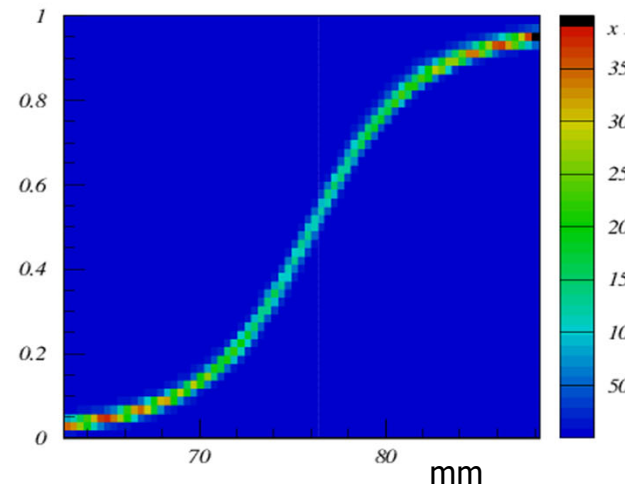
Time resolution vs PC-MCP1 voltage

MCP PMT readout: capacitive coupling vs. internal anodes

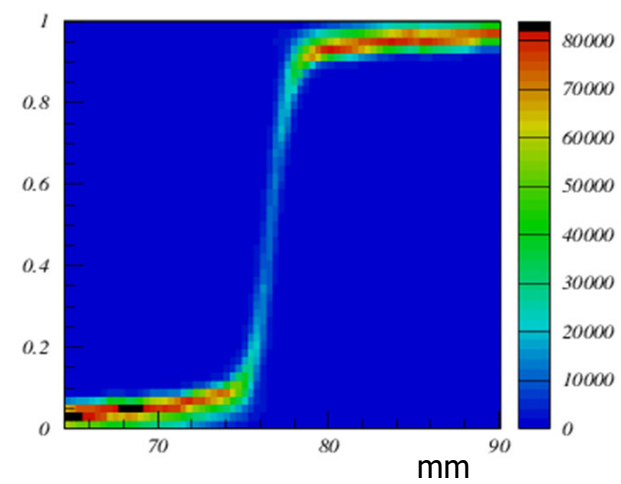
Secondary electrons spread out when traveling from the MCP-out electrode to the anode and can hit more than one anode → Charge sharing
Can be used to improve spatial resolution.



LAPPD (capacitive coupling through the backplane)



BURLE/Photonis PLANACON (internal anodes)



Fraction of the charge detected by the right pad as a function of red laser spot position

Capacitive coupling vs. internal anodes: signal spread comparison for two MCP PMTs with the same pad size, same range: charge sharing is more effective for capacitive coupling (spreads over larger area) - advantage or not: depends on the usage

Possible Future of Electron Multiplication

Tynodes (\rightarrow Time Photon Counter)

Transmission mode dynode \rightarrow tynode

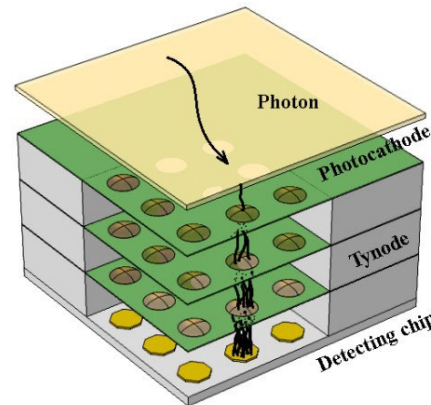
Fabrication of tynodes (MgO ALD, diamond) using MEMS technology

"Anode" is a CMOS chip (e.g., TimePix)

Very promising properties

Very compact; high B-field tolerance; very fast

Very low DCR; very good 2D spatial resolution

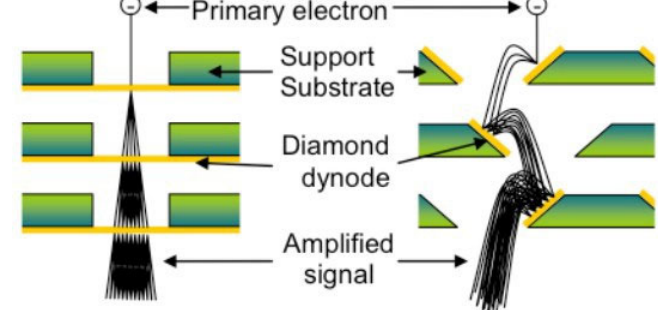


H. van der Graaf et al., NIM A847 (2017) 148

Transmission



Reflection



MCP-PMT with CMOS anode

Conceptual design for 4D detection of single photons

Hybrid concept: MCP-PMT where the pixelated anode is an ASIC (CMOS) embedded inside the vacuum

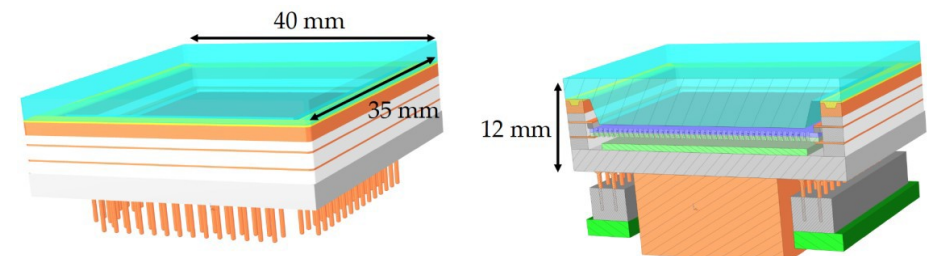
Prototype with Timepix4 ASIC as anode (array of 23k pixels)

Envisaged performance

<100 ps time resolution and 5-10 μm spatial resolution

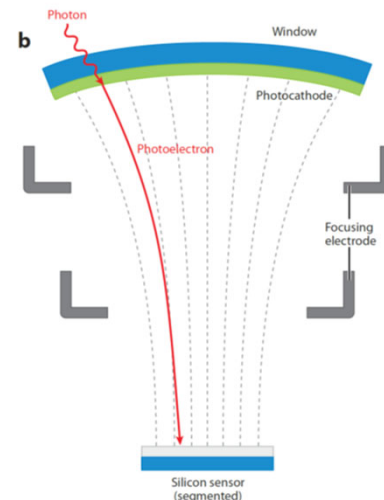
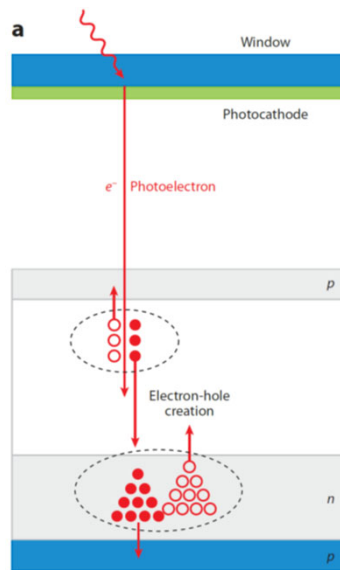
Rate capability of >100 MHz/cm² (<2.5 Ghits/s @ 7 cm² area)

Low gain ($\sim 10^4$) operation possible \rightarrow x100 lifetime increase



M. Fiorini, RICH2022

Hybrid photodetectors (HPD, HAPD)



Focusing and proximity focusing configurations

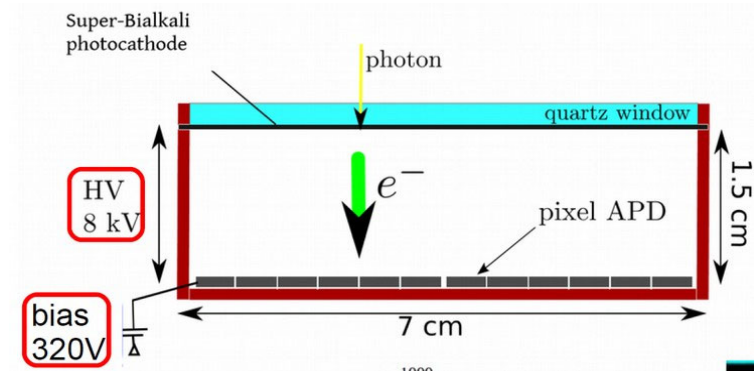


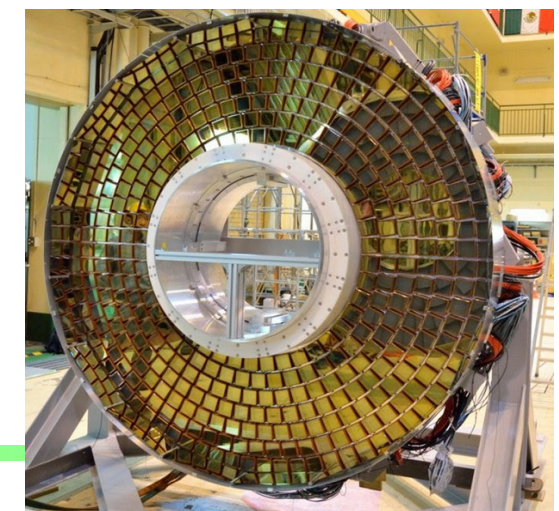
Photo-electron acceleration in a static electric field (8kV to 25 kV)

Photo-electron detection with

- Segmented PIN diode (HPD)
- Avalanche photo diode (HAPD)
- Silicon photomultiplier (VSiPMT)

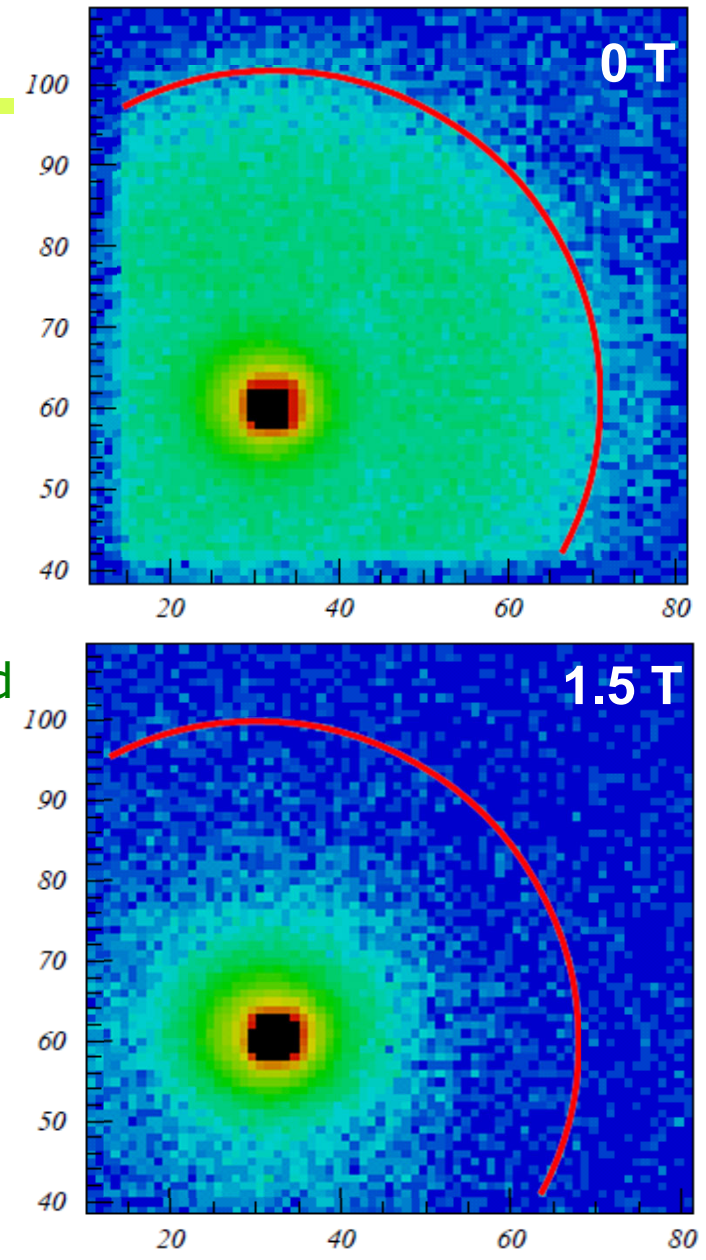
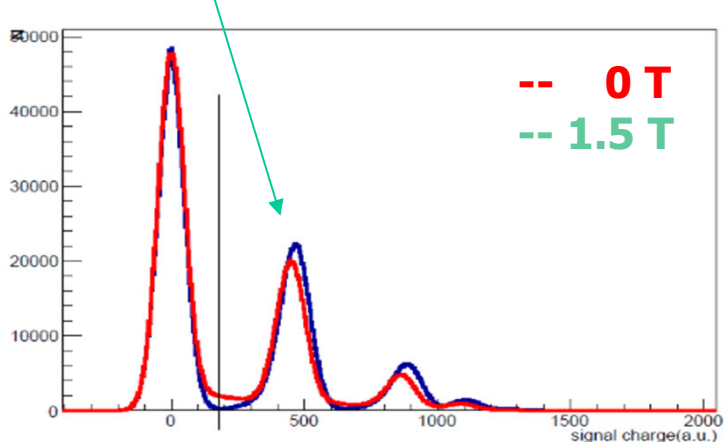
Employed on a large scale:

- HPD: RICH1+RICH2 of LHCb (Run 1+2), CMS HCAL
- HAPD: Aerogel RICH detector of Belle II



HAPD: photoelectron backscattering in magnetic field

- around 20% of photoelectrons back-scatter and the maximum range is twice the distance from photocathode to APD $\sim 40\text{mm}$
- in magnetic field (perp. to the HAPD window) scattered photoelectrons follow magnetic field lines and fall back to the same pad
- photoelectron energy is deposited at the same pad

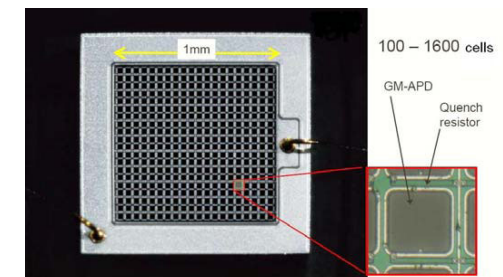
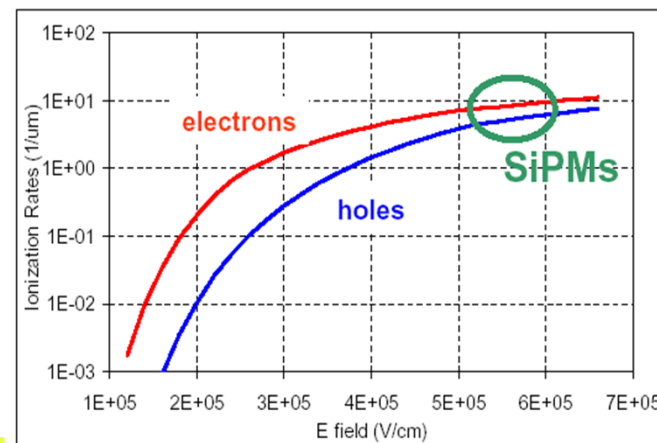
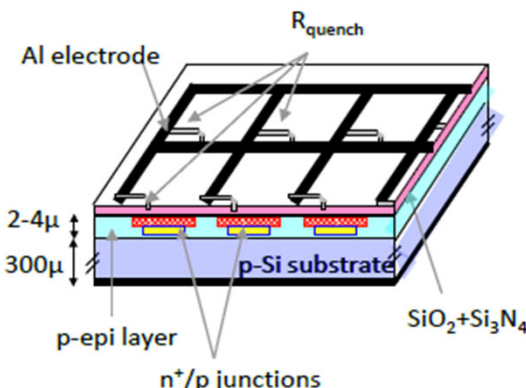


Solid state low light level photosensors: Silicon photomultipliers SiPM

An array of APDs operated in Geiger mode – above APD breakdown voltage (microcells or SPADs – single photon avalanche diodes)

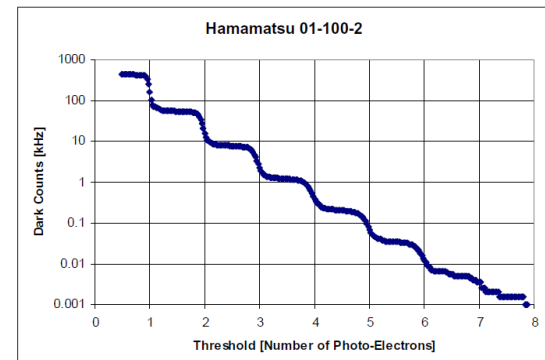
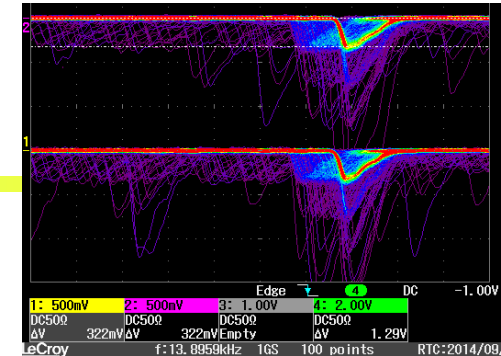
Detection of photons:

- absorbed photon generates an electron-hole pair
- an avalanche is triggered by the carrier in the high field region → signal
- voltage drops below breakdown and avalanche is quenched (passive or active quenching)
- each triggered microcell contributes the same amount of charge to the signal

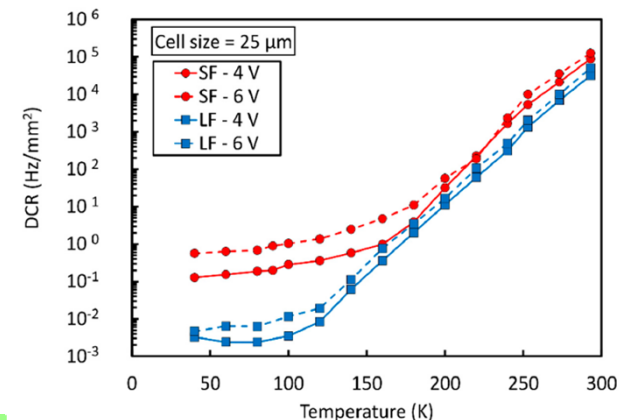


SiPM: noise

- dark counts are produced by thermal generation of carriers, trap assisted tunnelling or band gap tunnelling
- signal equal to single photon response
- typical rate went from $\approx 1\text{MHz}/\text{mm}^2$ to below $100\text{kHz}/\text{mm}^2$ for more recent devices
- roughly halved for every -8°C
- increases linearly with fluence
- optical cross-talk produced when photons emitted in avalanche initiate signal in neighbouring cell, reduced by screening – trenches
- after-pulses produced by trap-release of carriers or delayed arrival of optically induced carrier in the same cell



A. Gola et al. Sensors 19(2019)308



SiPM: parameter correlation

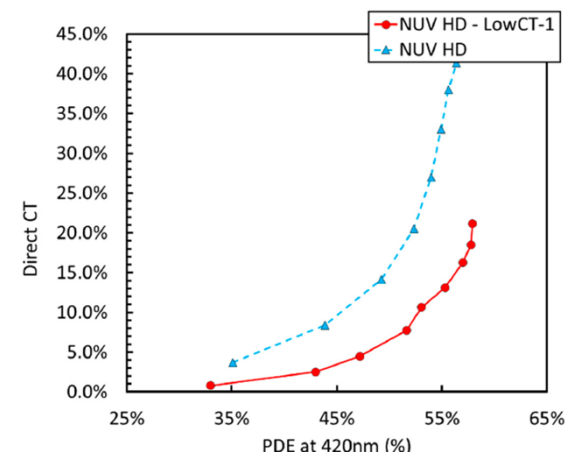
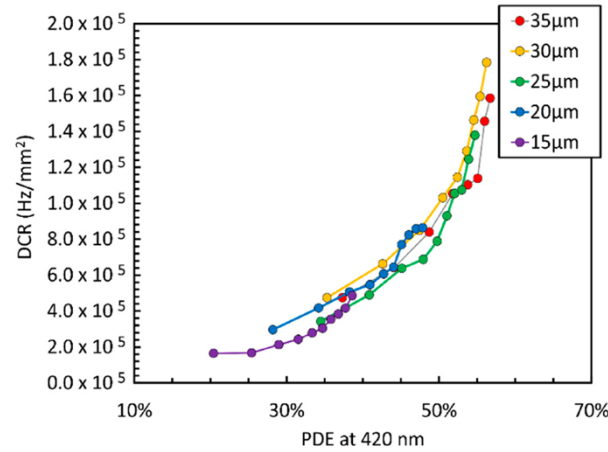
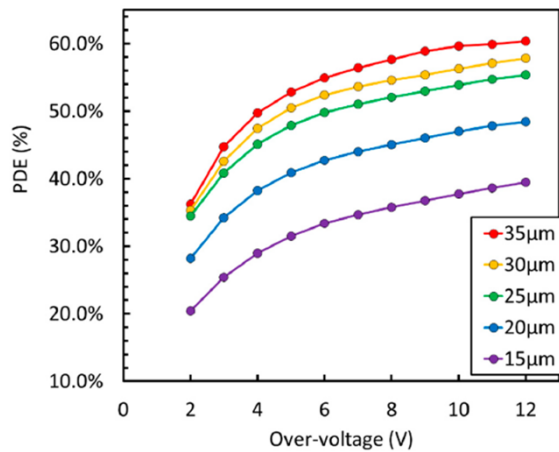
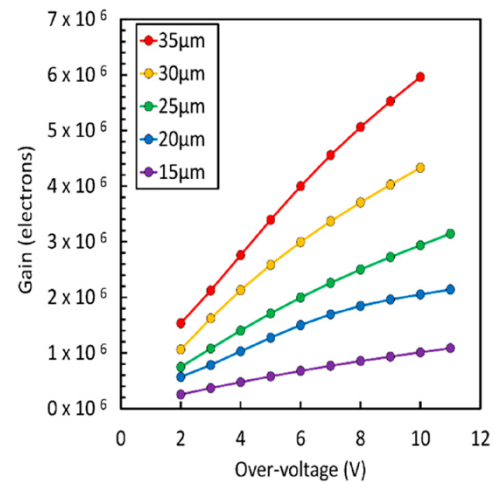
Higher overvoltage:

➤ higher field:

- higher avalanche trigger probability → higher PDE
- faster signal → better timing

➤ higher gain:

- better signal to noise (electronic)
- more optical cross-talk → higher ENF, worse timing
- more after-pulses

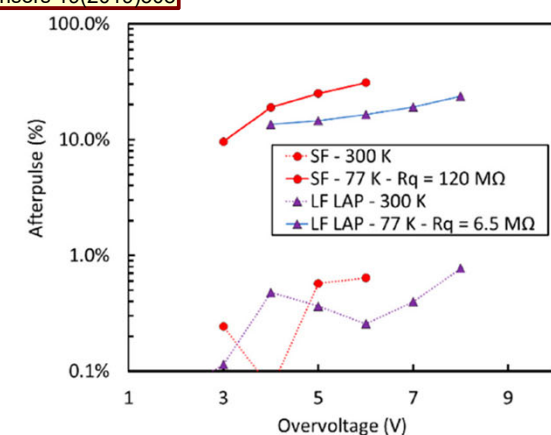
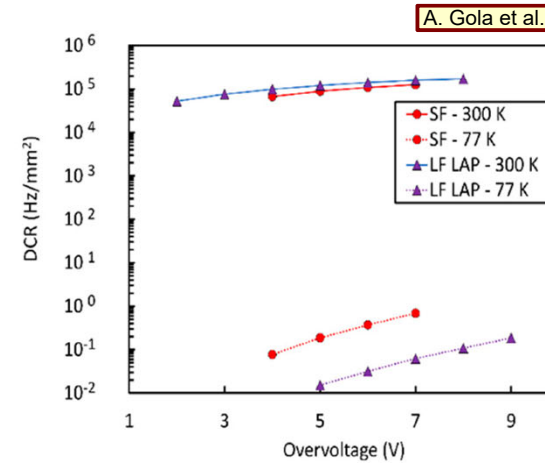
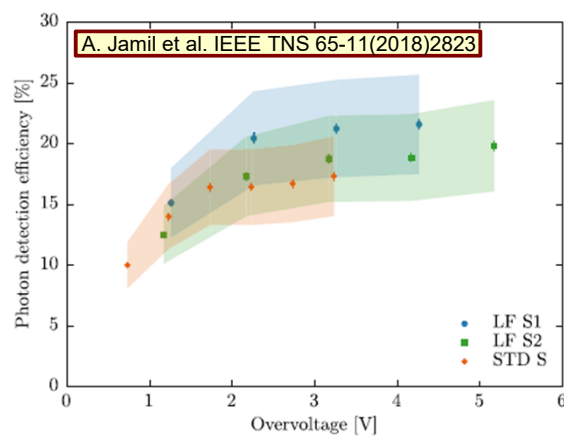
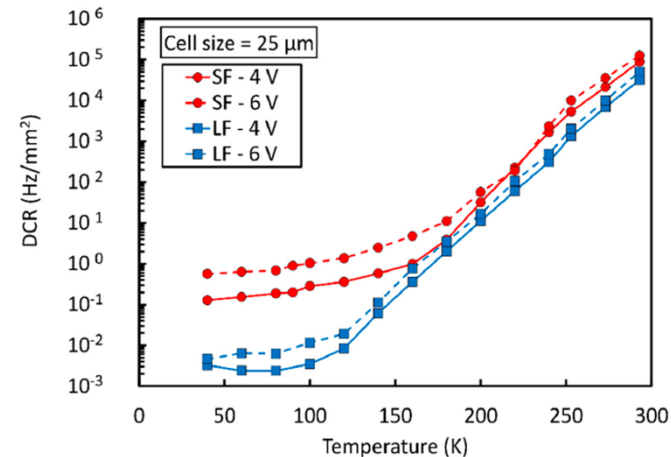


A. Gola et al. Sensors 19(2019)308

VUV SiPM for cryogenic applications

LAr, LXe applications:

- VUV sensitivity required:
 - 128 nm (LAr), 178 nm (LXe)
 - optimization of anti-reflective coating ARC
 - PDE $\approx 20\%$
- cryogenic temperatures:
 - low DCR $\approx 10\text{mHz/mm}^2$ dominated by band-band tunnelling, reduced by low-field avalanche region
 - higher after-pulse rate $\approx 10\%$



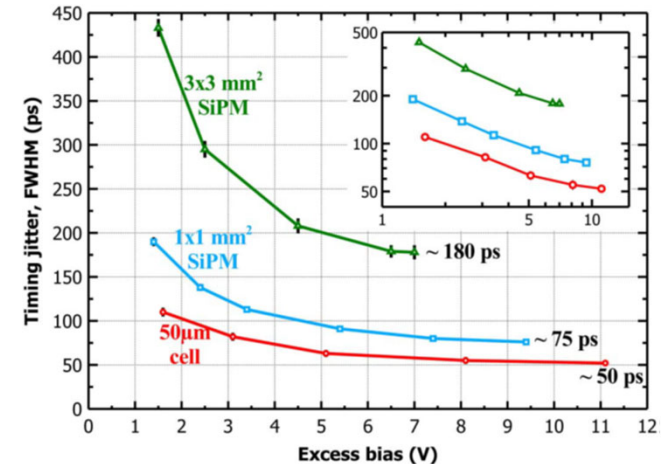
SiPM: single photon timing

Intrinsic TTS of SiPM microcells is extremely fast, < 20 ps for single microcells (SPAD), but timing deteriorates for larger devices. The main contributions:

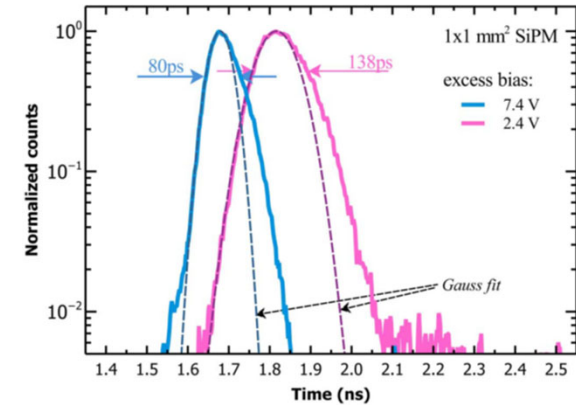
- nonuniformity within microcell (edges)
- spread between microcells
- overall SiPM capacitance
- λ dependence - tails

Comparison of timing properties for single 50 μm SPAD, 1 \times 1 mm² and 3 \times 3 mm² SiPMs with the same SPAD for microcells:

- timing improves with higher overvoltage – larger pulses, at the expense of increased SiPM noise
- best timing resolutions for single cell signals are $\sigma \approx$ 21 ps, 32 ps and 77 ps
- TTS deterioration mainly due to a larger overall capacitance \rightarrow reduced signal slope, $\sigma_t \approx \sigma_{el.} \left(\frac{dU}{dt} \right)^{-1}$



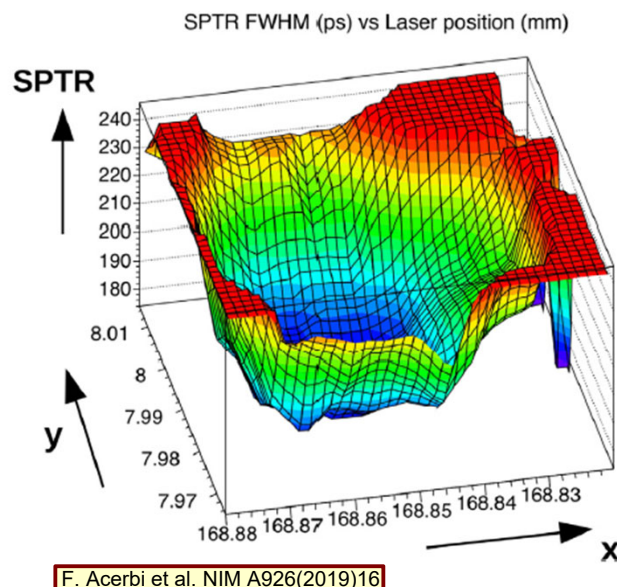
F. Acerbi et al. IEEE TNS 61(2014)2678



SiPM: timing variation

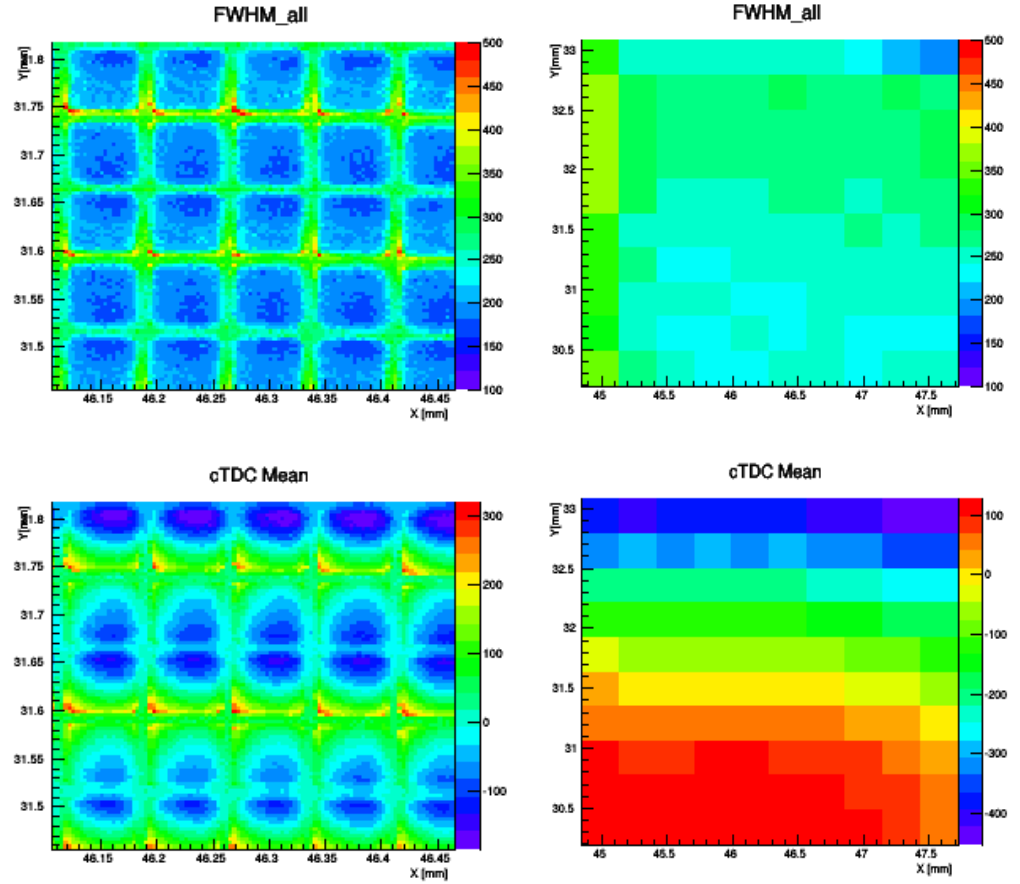
Variation of TTS over the device surface can contribute to overall time spread:

- variation within micro-cell
- variation for different micro-cells



KETEK PM3375TS-SBO (early design)

S. Korpar et al. @IEEE 2015

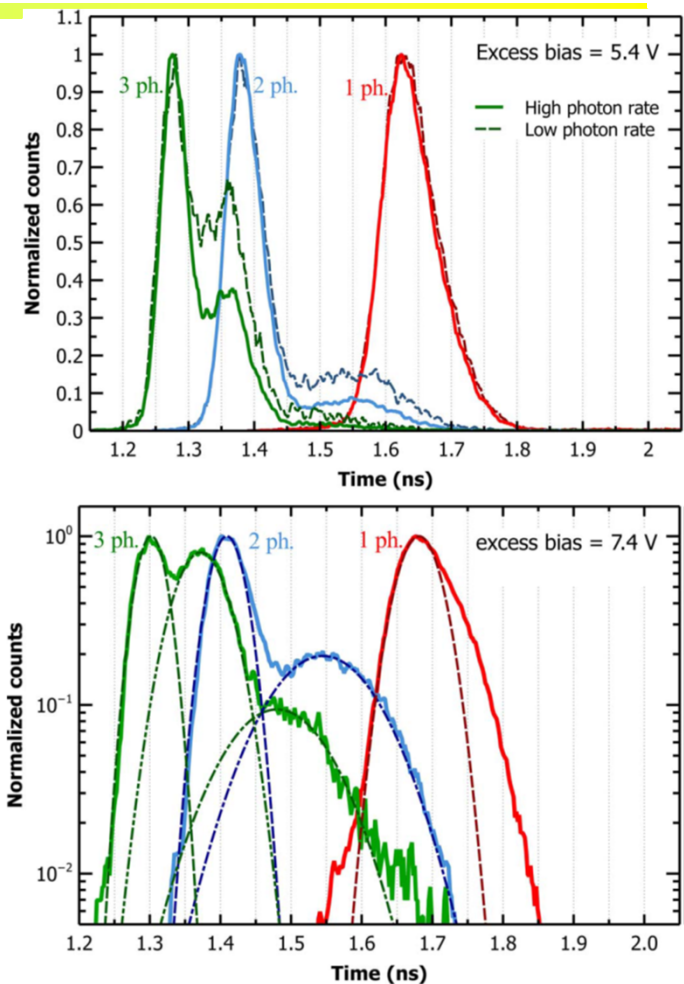


FBK: Masking of outer regions of micro-cells: Improve signal peaking and mask areas of micro-cell with worse timing

SiPM: timing for multi-cell signals

Optical cross-talk contribution to multi-cell signals spoils timing distribution – does not scale with $\frac{1}{N^{1/2}}$:

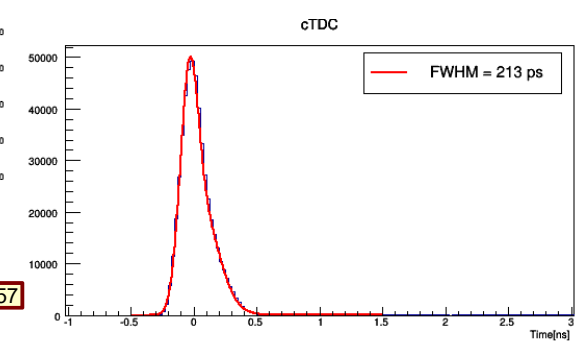
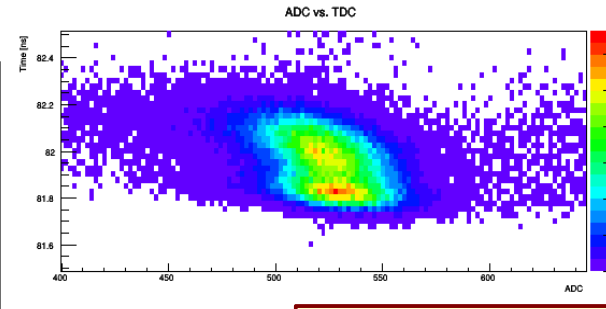
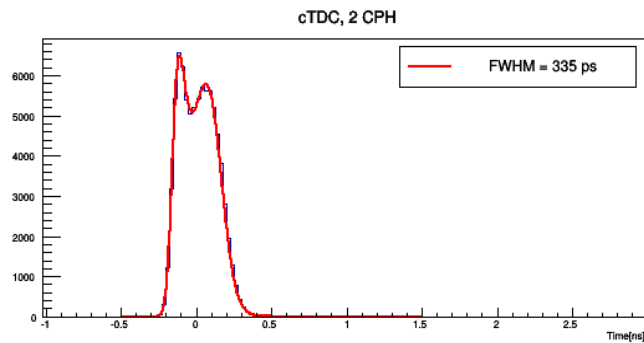
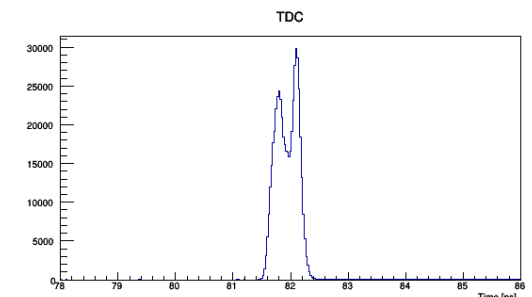
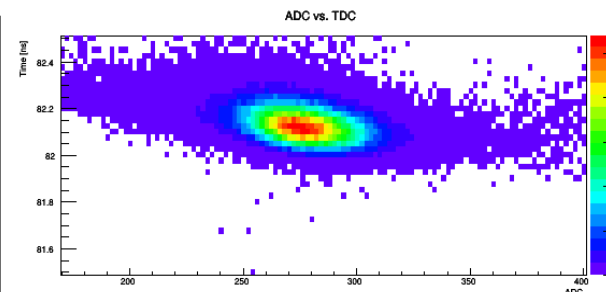
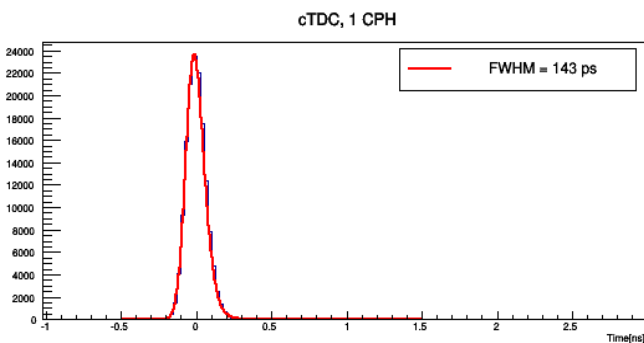
- two components for 2-micro-cell signals:
 - double photon events – proper scaling
 - single photon with cross-talk, timing somewhere between single and double micro-cell signals and resolution is worse
- ratio between contributions changes with light intensity confirming optical cross-talk origin
- even more components for multi-micro-cell signals



[F. Acerbi et al. IEEE TNS 61(2014)2678]

SiPM: timing test with pico-second laser

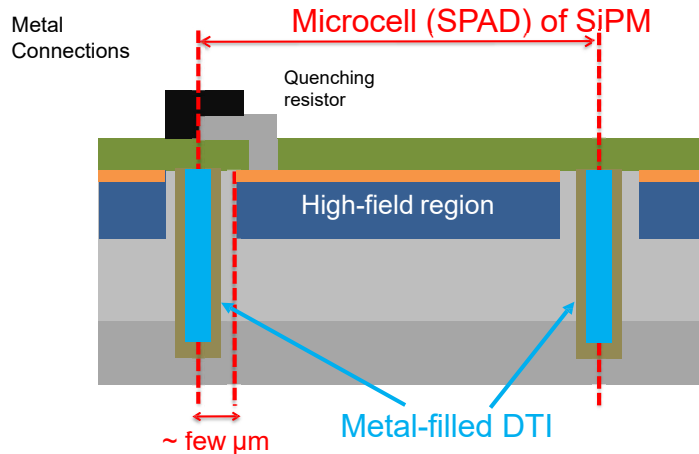
- AdvanSiD SiPM ASD-NUV3S-P-40
- OV=6V, T=-2n5°C
- blue laser $\lambda = 408\text{nm}$, $\sim 35\text{ps FWHM}$



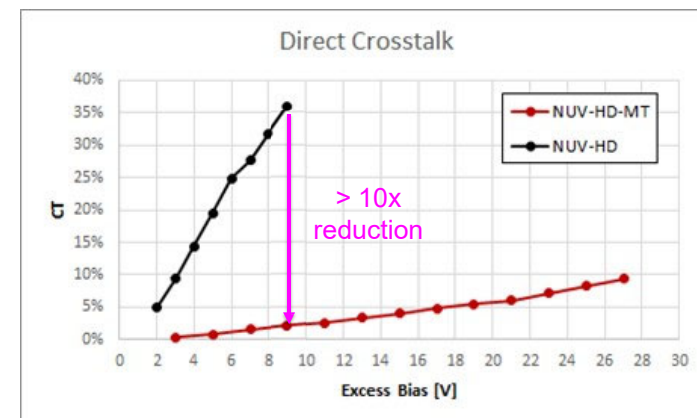
Reduction of optical crosstalk

Starting from the NUV-HD technology, FBK and Broadcom jointly developed the NUV-HD-MT technology, adding metal-filled deep trench isolation to strongly suppress optical crosstalk.

Other changes: low electric field variant, layout optimized for timing.



Conceptual drawing of the NUV-HD-MT, with the addition of metal-filled Deep Trench Isolation.



Reduction of optical crosstalk probability in NUV-HD-MT, compared to the “standard” NUV-HD. Measurement without encapsulation resin, i.e. only considering internal crosstalk probability.

A. Gola, RICH2022

Light concentrators

At the device level (lenses, Winston cones):

- reduce active area – reduce DCR (tolerate higher fluences)
- use smaller faster devices

At the micro-cell level (micro-lenses, diffractive lenses, meta lenses):

- compensate for low fill factor – small cells, dSiPM
- concentrate light in cell centre – better timing

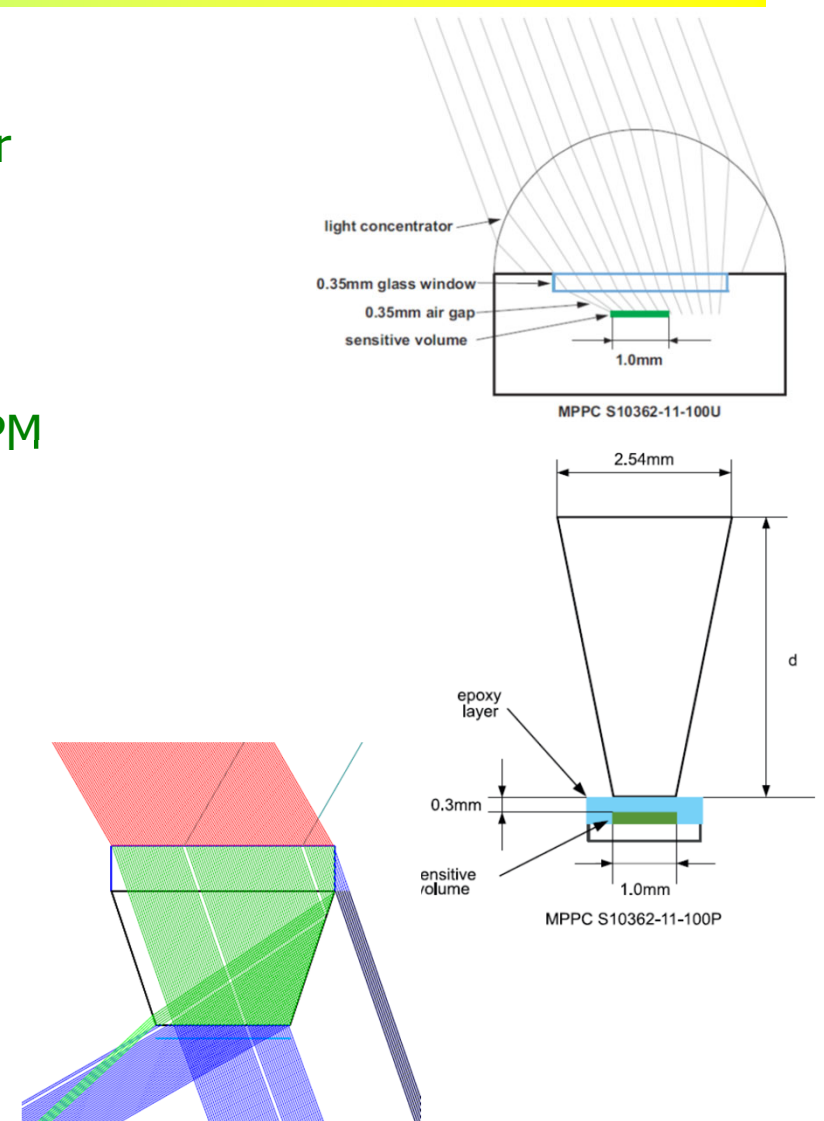
Higher concentration – narrower angular acceptance

Imaging light concentrators:

- smaller photon impact angles on the sensor
- can be used with position sensitive arrays

Non-imaging light concentrators:

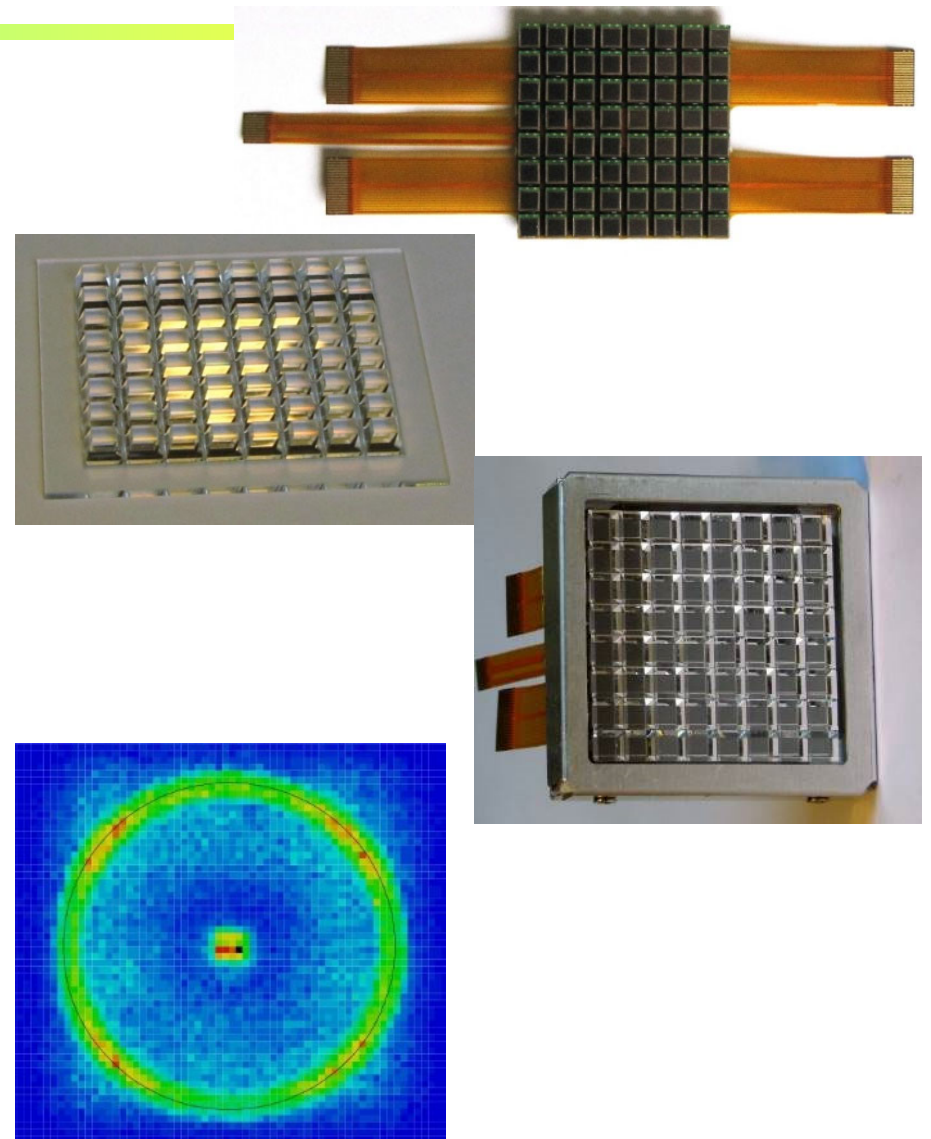
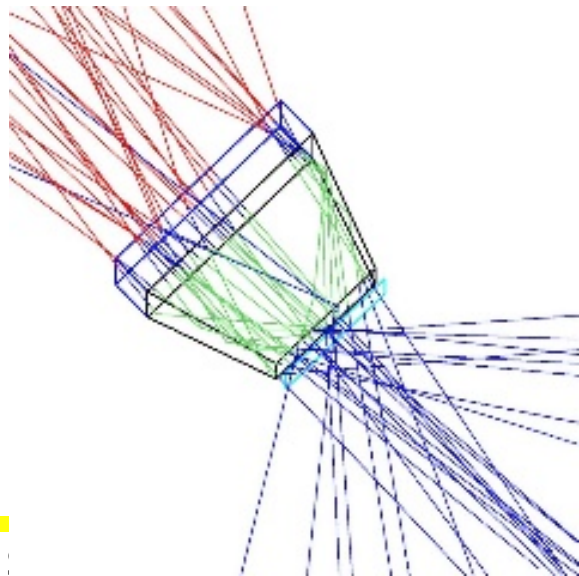
- larger photon impact angles on the sensor – directly coupled to sensor



SiPM RICH with light concentrators

RICH photon detector module prototype:

- Hamamatsu 64 channel MPPC module S11834-3388DF, 8 × 8 array of $3 \times 3 \text{ mm}^2$ SiPMs @ 5 mm pitch
- matching array of quartz light concentrators used
- two 20 mm thick aerogel tiles in focusing configuration ($n = 1.045, 1.055$)
- tested in 5 GeV electron beam at DESY

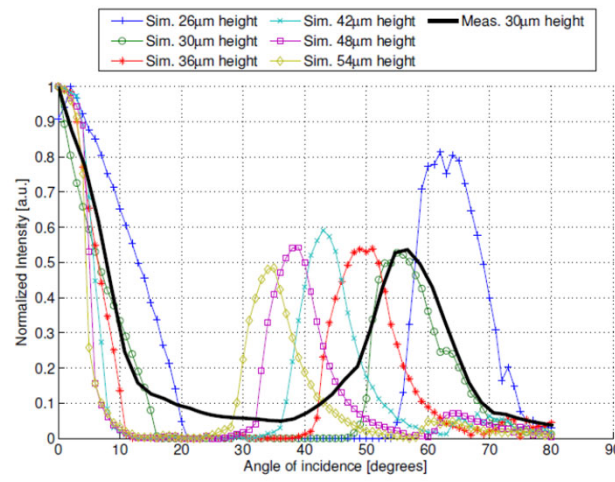
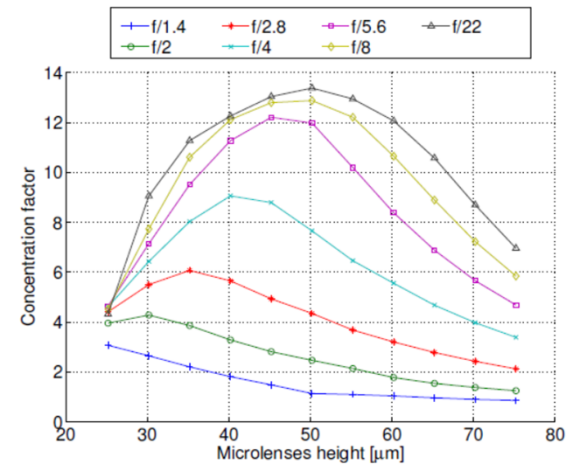
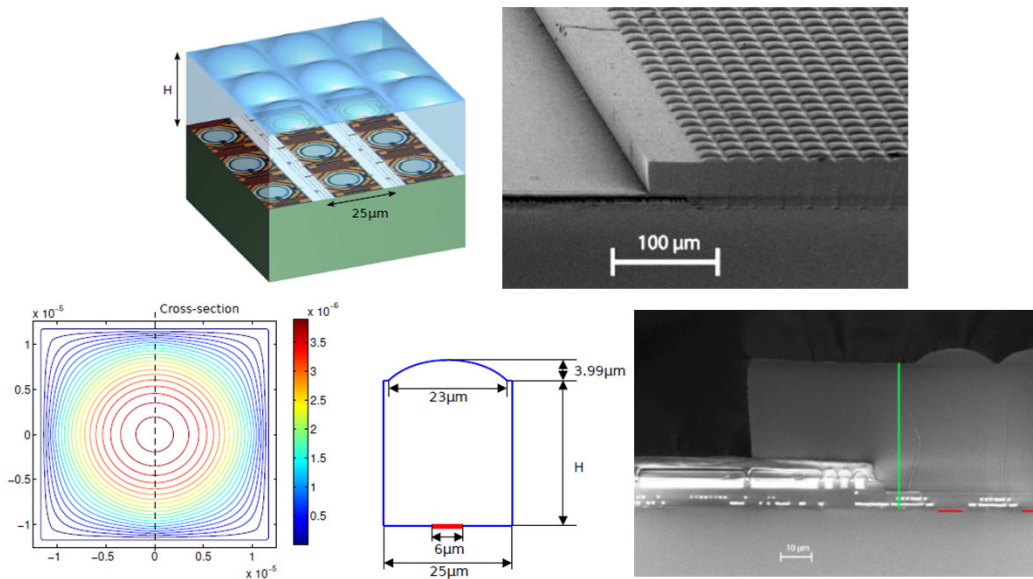


E. Tahirović et al., NIM A787 (2015) 203

Microlenses

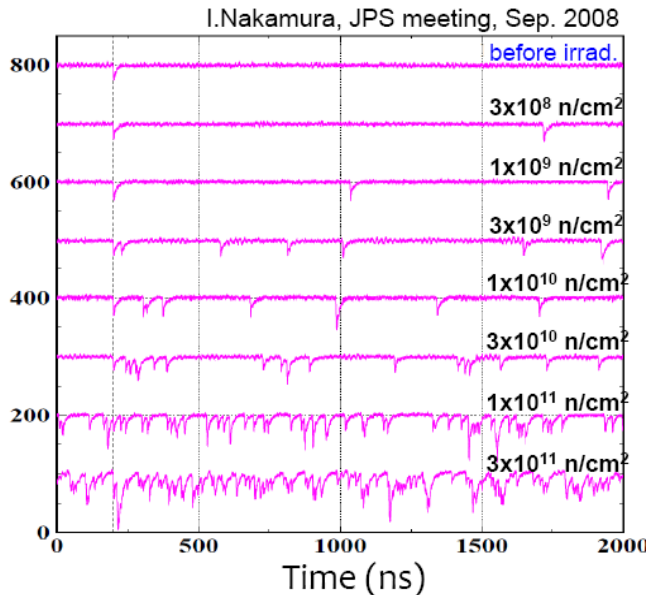
Micro-lens array coupled to SPAD array

- CMOS SPAD array, 128x128 $6\mu\text{m}$ diameter
@ $25\mu\text{m}$ pitch – 5% fill factor
- matching polymer plano-convex micro-lens array



J.M. Pavia et al. Opt.Exp. 22-4(2014)4202

SiPMs: Radiation damage



Show stopper at fluences above $\sim 10^{11}$ in case single (or few) photon sensitivity is required!

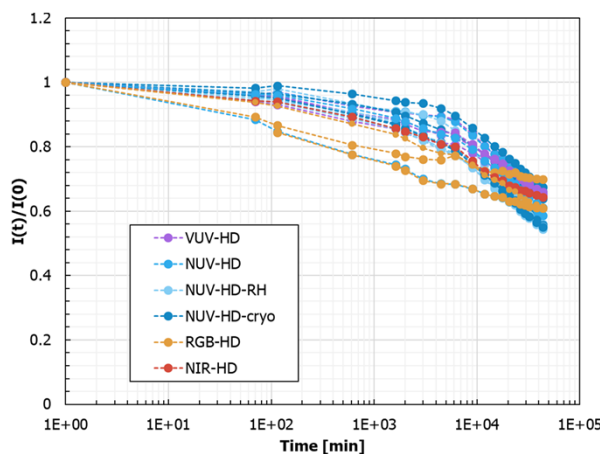
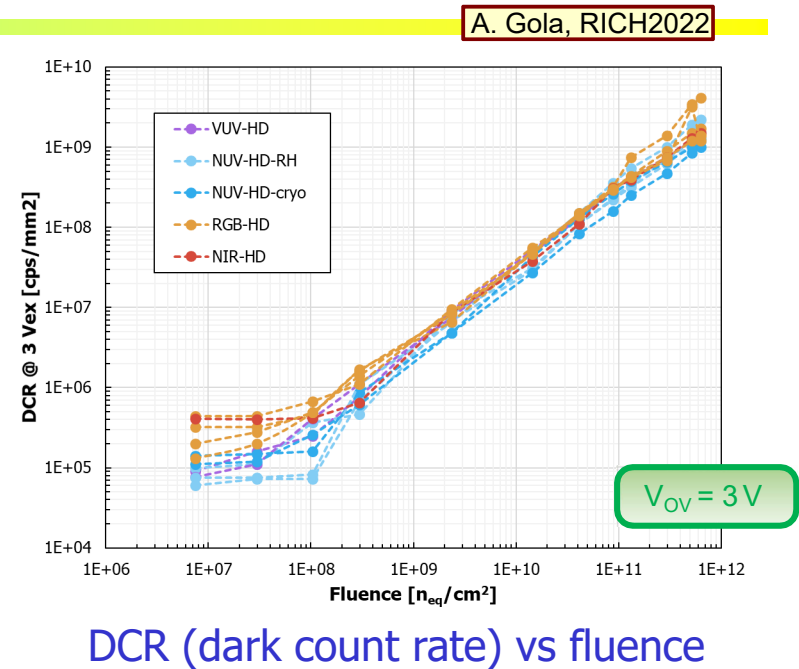
(e.g. expected fluence in the ARICH area of Belle II: 2-20 $10^{11} \text{ n cm}^{-2}$)

- Use of wave-form sampling readout electronics
- Operating the SiPMs at lower temperature
- Annealing periodically (annealing at elevated temperature is preferred)
- Reducing recovery time to lower cell occupancy
- Radiation resistant SiPMs, other materials?

SiPMs: Radiation damage

Beyond $10^7 \div 10^8 \text{ n}_{\text{eq}}/\text{cm}^2$ little correlation between the DCR before and after irradiation:

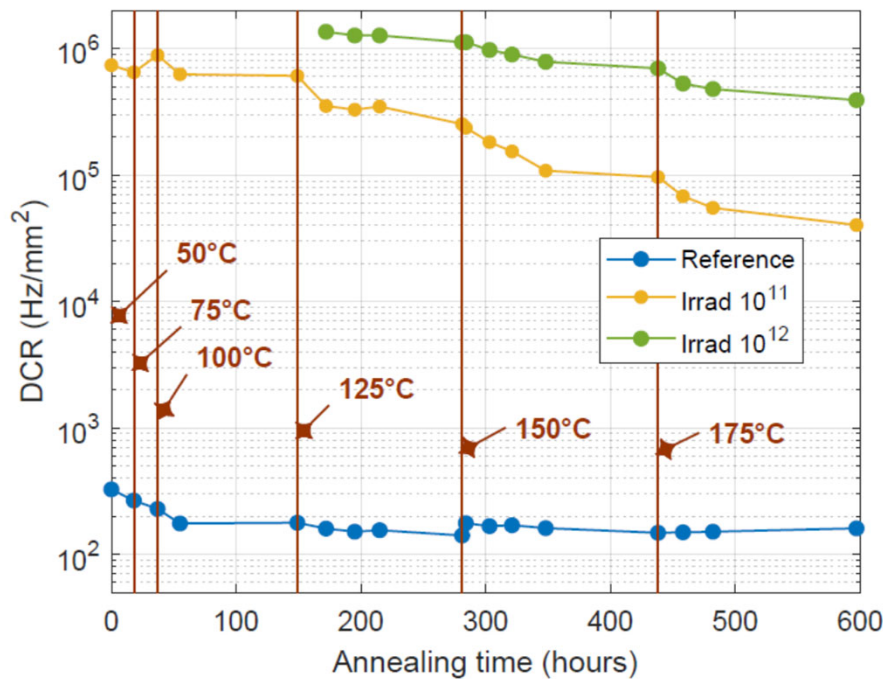
- All technologies seem to “converge” towards similar values
- Independence of bulk damage from contaminants in the SiPM starting material?



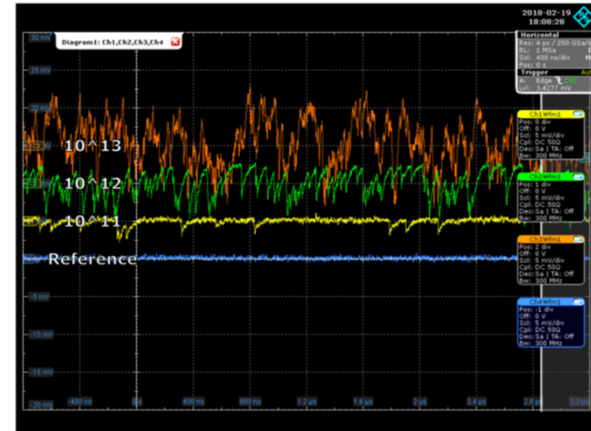
Room temperature annealing ($20\text{-}25^\circ\text{C}$) for samples irradiated to $6.4 \cdot 10^{11} \text{ 1 MeV n}_{\text{eq}}/\text{cm}^2$
Little effect, knee point at around $1.5 \cdot 10^3 \text{ min} (\sim 1 \text{ day})$

SiPMs: Radiation damage, annealing at elevated temperatures

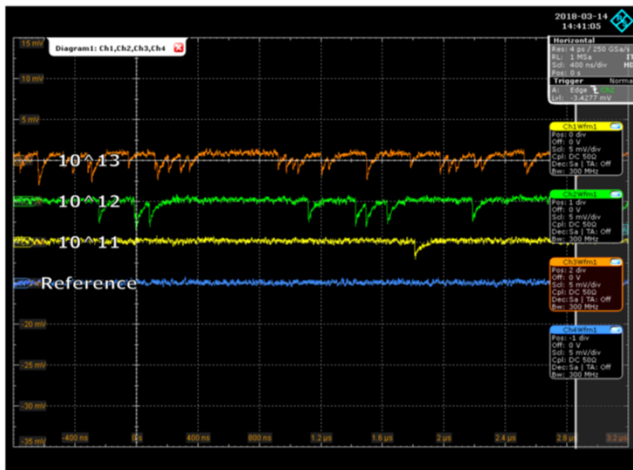
Dark counts at -30C of a Hamamatsu S13360-1350CS
SiPMs: non irradiated (blue) and irradiated up to 10^{11} (yellow), 10^{12} (green) and 10^{13} (orange) n_{eq}/cm^2



M. Calvi et al., NIMA 922 (2019) 243-249

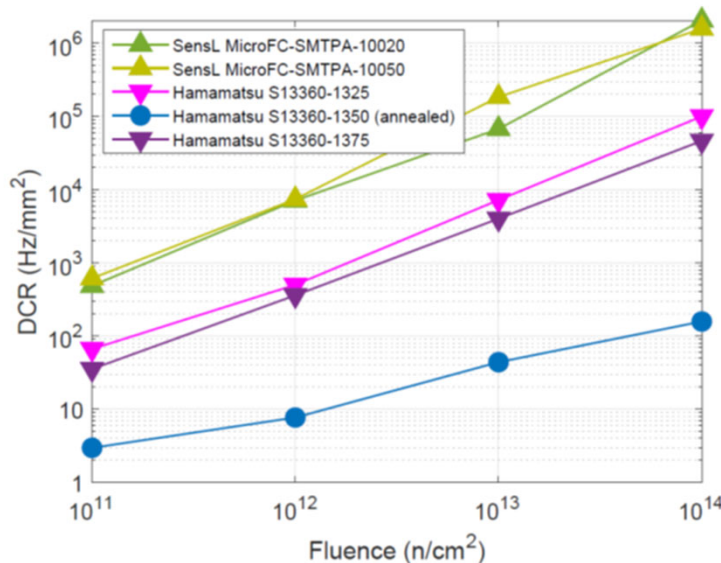


annealing



SiPMs: Radiation damage, annealing at elevated temperatures

M. Calvi et al., NIMA 922 (2019) 243-249



DCR at 77 K versus neutron fluence

Blue circles: annealed sample

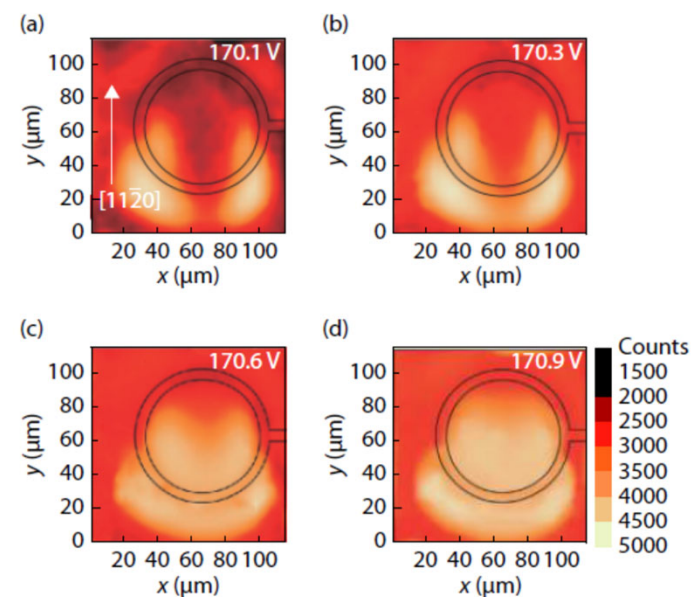
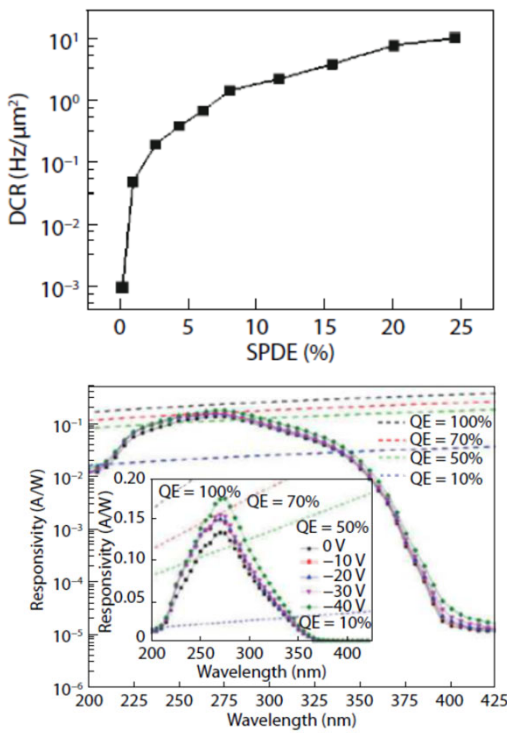
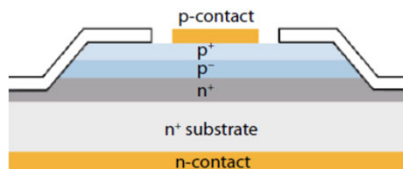
→ Annealing helps also at 77 K

New materials

- new higher band gap materials - possibly lower DCR - higher radiation resistance, higher temperature
- (V)UV sensitive
- high dark count rate – dominated by trap assisted tunnelling

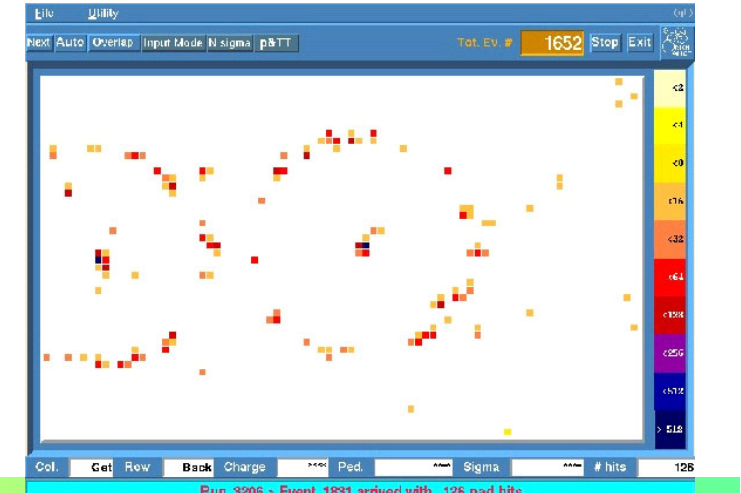
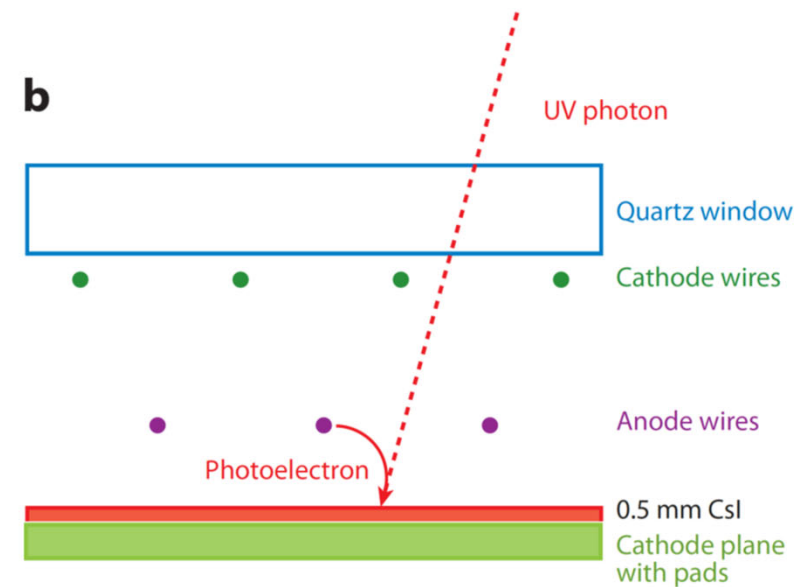
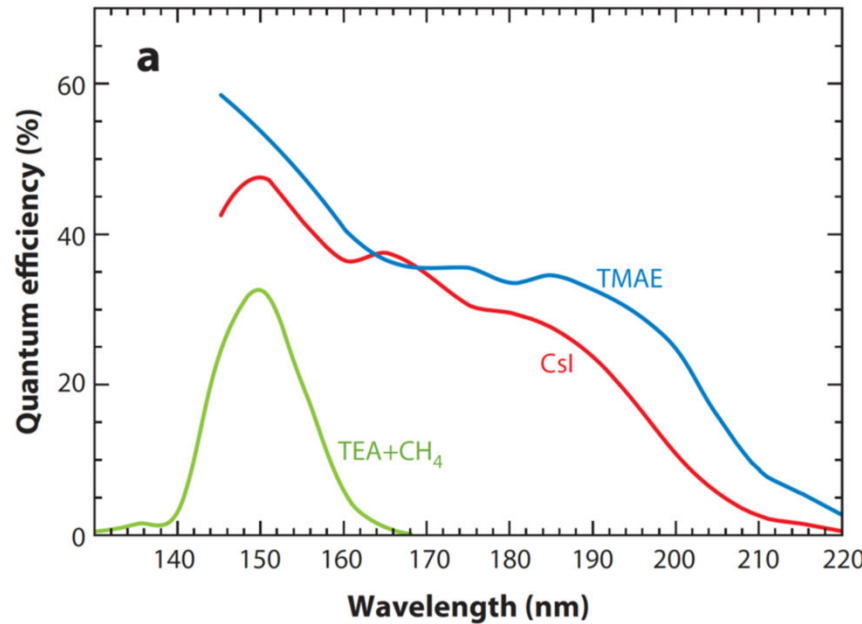
4H-SiC:

- $E_g = 3.26$ eV
- PDE $\approx 10\%$
- DCR > 1 MHz/mm²
- nonuniform response



L. Su et al. J. Semicond. 40(2019)121802

Gas based photon detectors



Standard photosensitive substance: CsI
evaporated on one of the cathodes.
Large scale application: $\sim 11 \text{ m}^2$ ALICE RICH

Gas based photon detectors: recent developments

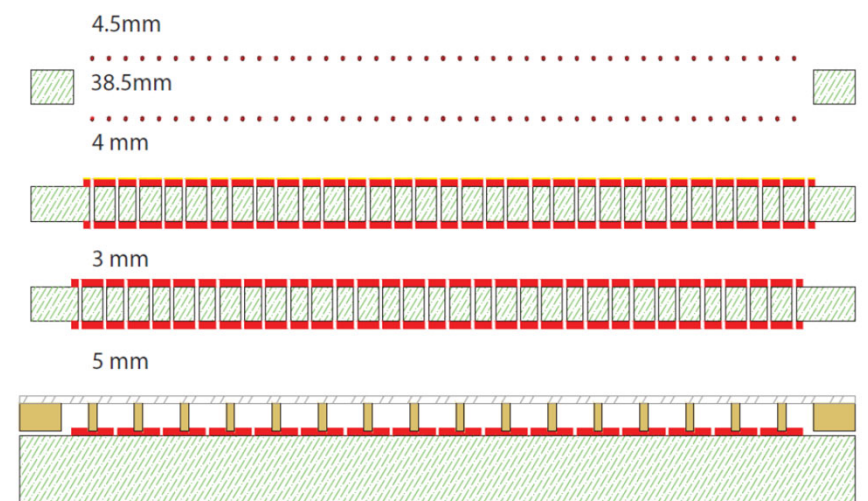
Instead of MWPC:

- Use chambers with multiple GEM or thick GEM (THGEM) gas amplification stages with transm. or refl. photocathode
- COMPASS RICH: trans. photocathode and 2x THGEM + MicroMegas

S. Dalla Torre, NIM A 970 (2020) 163768

Ion damage of the photocathode:

blocking ions – non-aligned GEM holes



New developments:

- Smaller pads
- Novel photocathode material: nano-diamond layer

Summary and outlook

Next generation of experiments in particle physics: faster timing, wider spectral range and improved radiation tolerance.

Many new interesting developments underway, in particular in SiPMs and MCP-PMTs – not all of them could be covered in this talk.

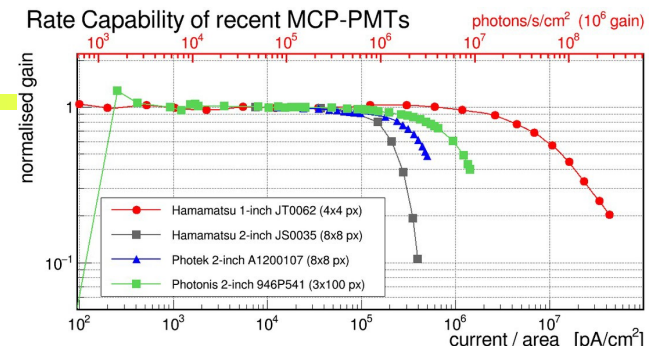
A detector R&D collaboration (DRD4) is being set-up to facilitate collaboration in this area of research, expected to start in January 2024.

Back-up slides

Rate Capability

MaPMT

MaPMT R13742: no gain loss to up 10 MHz/mm²



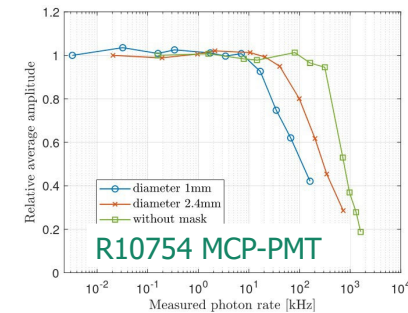
MCP-PMTs

Gain decreases at high photon rates

2-inch MCP-PMTs: ~1 MHz/cm² (with 10⁶ gain)

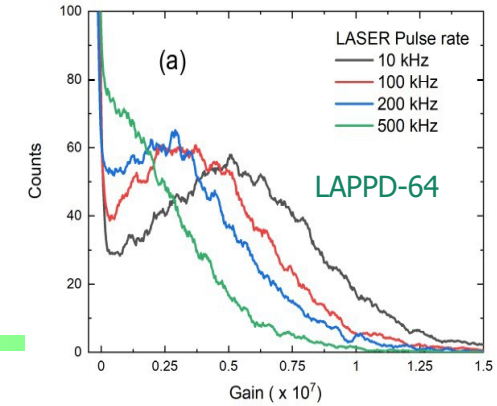
1-inch Hamamatsu R10754 PMTs: ≥10 MHz/cm²

8-inch LAPPD-64: ~100 kHz at 4.6 mm Ø laser spot



Improving the rate capability in MCP-PMTs

- Lower MCP resistance (ranging at tens of MΩ)
- Lower capacitance - subdivision of MCP layers into smaller partial areas; the second MCP layer was divided in the previous version of Hamamatsu tubes
- Low gain operation (for single photon detection) - may be possible with amplifiers included directly in the anode (e.g., monolithic or CMOS designs)



Radiation Tolerance

MaPMT

Recently tested for CBM (H12700 and H8500)

Irradiation dose up to $3 \times 10^{11} \text{ n/cm}^2$ and **150 Gy** gammas

Few kHz increase of DCR but recovers after few months

UV glass: 1-2% transmission loss @ 400 nm up to 1 kGy

No negative effects on gain and pulse height spectrum

Neutron activation of Kovar metal alloy is a minor effect

H(A)PD

Radiation tolerance dominated by silicon

detector Intensively studied for 144ch HAPD

for ARICH @Belle II

Basically **no QE loss at $5 \times 10^{11} \text{ n/cm}^2$**

Increase of APD leakage current leads to significantly worse S/N ratio: ~17 before, ~3 after irradiation

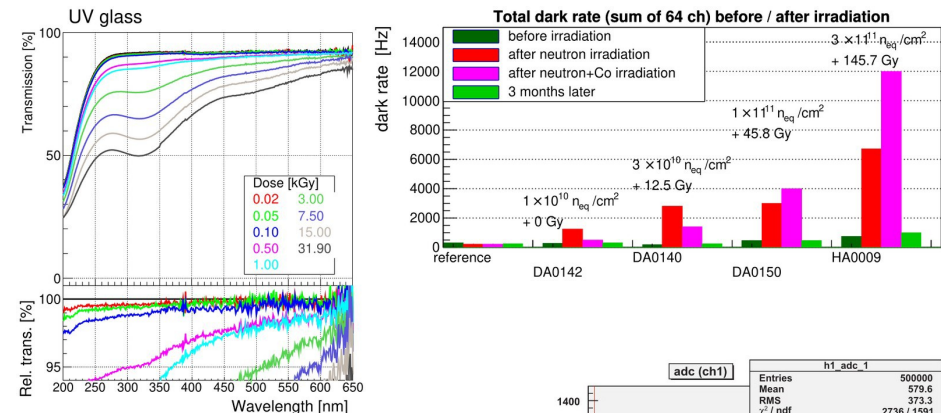
S/N ratio partly regained by adjusted readout parameters

MCP-PMT

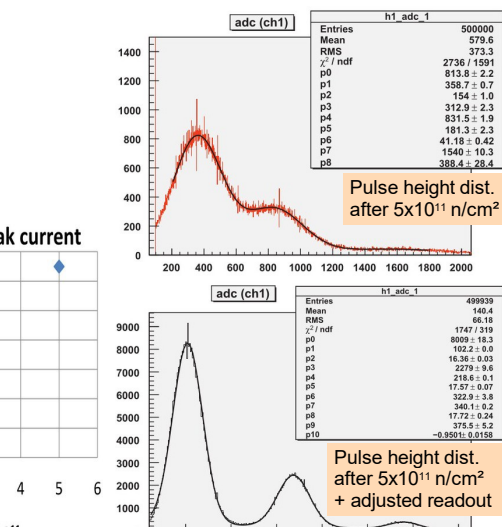
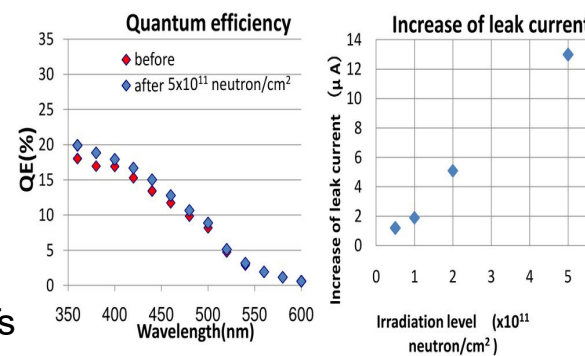
Entrance window: should be similar to other PMTs

MCPs: currently no data

C. Pauly et al., NIM A1040 (2022) 167177



.S. Shiizuka, Talk at VCI 2010

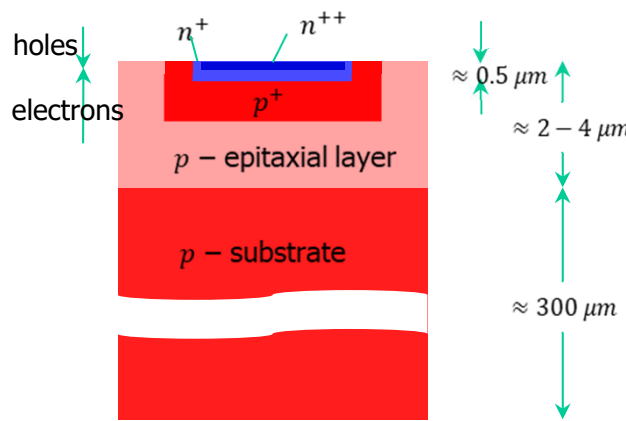


I. Adachi, NIM A639 (2011) 103

SiPM: p-on-n vs. n-on-p

n-on-p: green/red light sensitive:

- electrons drift to Geiger region from substrate and holes from surface side
- higher dark count rate – most of the thermally generated carriers arriving to Geiger region are electrons



p on n - green/blue light sensitive:

- electrons drift to Geiger region from surface and holes from substrate side
- lower dark count rate – most of the thermally generated carriers arriving to the Geiger region are holes

